# Ocean Spray

Fabrice Veron

School of Marine Science and Policy, University of Delaware, Newark, Delaware 19716; email: fveron@udel.edu

Annu. Rev. Fluid Mech. 2015. 47:507–38

The *Annual Review of Fluid Mechanics* is online at fluid.annualreviews.org

This article's doi: 10.1146/annurev-fluid-010814-014651



## Keywords

waves, heat flux, tropical cyclones

## Abstract

Ocean spray consists of small water droplets ejected from the ocean surface following surface breaking wave events. These drops get transported in the marine atmospheric boundary layer, in which they exchange momentum and heat with the atmosphere. Small spray droplets are transported over large distances and can remain in the atmosphere for several days, where they will scatter radiation; evaporate entirely, leaving behind sea salt; participate in the aerosol chemical cycle; and act as cloud condensation nuclei. Large droplets remain close to the ocean surface and affect the air-sea fluxes of momentum and enthalpy, thereby enhancing the intensity of tropical cyclones. This review summarizes recent progress and the emerging consensus about the number flux and implications of small sea spray droplets. I also summarize shortcomings in our understanding of the impact of large spray droplets on the meteorology of storm systems.

## 1. INTRODUCTION

**ABL:** atmospheric boundary layer

Sea spray, or ocean spray, comprises liquid droplets ejected from the sea surface generally due to breaking waves and related phenomena, such as bubble entrainment and whitecaps. The ejected droplets contain seawater as well as biological and chemical constituents from nonmarine sources. The spray composition is usually considered to be similar to that of bulk seawater, although water vapor exchange with the atmosphere and chemical reactions subsequent to spray formation will influence and change the composition. Once ejected from the ocean surface, spray drops are transported and dispersed in the marine atmospheric boundary layer (ABL), in which they interact and exchange momentum, heat, and moisture with the ambient atmosphere at rates that are relatively well described by fluid dynamics and thermodynamics.

Marine aerosols, which include both liquid and solid particles of marine origin, span a large size range, from radii of a few nanometers for sea salt particles to several millimeters for the larger spray droplets. The smaller particles have residence times of days to weeks. They disperse globally and interact in the global atmospheric aerosol cycle, in which they may participate in atmospheric chemical reactions or act as nucleation sites for clouds (Andreae & Rosenfeld 2008) and fog. Precipitation is in fact the primary deposition mechanism for these particles, although there is some debate as to whether dry or wet deposition is the dominant mechanism for atmospheric sea salt (Textor et al. 2006). The smallest spray droplets (of sizes on the order of nanometers) can also have chemical compositions that are significantly different from that of bulk seawater because their production mechanism might accumulate hydrophobic matter or surface-active material. Small marine aerosols scatter short-wave radiation, decreasing the amount of solar radiation reaching the ocean's surface by $O(1–5)\,\mathrm{W\,m^{-2}}$ (Lewis & Schwartz 2004), or absorb long-wave radiation. Sea salt particles represent approximately 90% of the aerosols in the marine boundary layer, almost half of the total natural aerosol flux, and more than one-third of the global total flux (Seinfeld & Pandis 1998). Estimates of the global emission of sea salt are on the order of $10^{12}$–$10^{14}$ kg per year (Textor et al. 2006). Consequently, there has been renewed interest in the past decade or so in the smallest sea spray droplets and their contribution to global and regional climates. Despite recent progress, the role of small marine aerosols in the global aerosol flux remains unclear.

Comparatively, our understanding of the role of the larger sea spray droplets is not significantly better. The larger droplets remain suspended in the atmosphere from fractions of a second to several minutes and typically settle back into the ocean under the effect of gravity. In fact, these droplets transfer heat and momentum with the atmosphere through direct exchange (Andreas 1992, 2004; Edson & Fairall 1994; Fairall et al. 1994; Andreas et al. 2008). The magnitude of these exchanges is still under debate, but it is presently thought that the sensible and latent fluxes directly attributed to the sea spray may be critical in the development of large tropical storm systems (Andreas & Emanuel 2001, Andreas 2011, Bao et al. 2011, Bianco et al. 2011). However, large uncertainties linger because these spray-mediated heat fluxes depend strongly on the rate of sea spray droplet formation at the surface. For large spray drops, the formation process is poorly understood; therefore, the formation rate of large sea spray droplets is not adequately described. In turn, it is very difficult to evaluate the spray feedback effects (i.e., the influence of the spray-mediated fluxes on the total air-sea fluxes).

In this review, I focus on the primary aqueous sea spray droplets that are directly ejected from the sea surface. These droplets, as shown below, have radii that are generally larger than $O(0.01)$ μm. The reader interested in dry marine aerosols and sea salt aerosol is referred to a comprehensive monograph by Lewis & Schwartz (2004) and recent reviews by de Leeuw et al. (2011) and O'Dowd & de Leeuw (2007), the latter containing significant information about the

chemical implications of sea spray, which are not covered here. De Leeuw et al. (2011) described small sea spray droplets and the resulting sea salt aerosols. Thus, when appropriate, I bias this review toward the larger spray droplets.

This review is written for a wide audience with good knowledge of general fluid mechanics. It should be considered as a starting point on the subject rather than an exhaustive review. The interested reader is encouraged to go well beyond the literature cited therein. I offer here sincere apologies to the sea spray enthusiast whose work I have overlooked, whether as a result of editorial constraints or by my own omission.

**Film drop:** seawater droplet expelled in the air when a bubble cap shatters

**Jet drop:** seawater droplet ejected from the sea surface when a bubble cavity collapses

**Spume drop:** seawater droplet mechanically torn off from the crest of a breaking wave

## 2. SPRAY GENERATION MECHANISMS

Spray droplets are formed through two main pathways. The first one occurs when bubbles, previously entrained in the water column by breaking waves, rise to the surface and burst. This bursting event is a very energetic phenomenon that in turn creates film and jet drops through two different processes. Film drops are generated when the bubble bursts and the surface film shatters; the receding rims become unstable and eject $O(10–100)$ small droplets. Jet drops are generated when the bubble cavity collapses and shoots up a central jet that also becomes unstable and breaks up into several daughter droplets. The second pathway generates so-called spume drops and occurs when the wind shear at the surface is sufficiently high for water droplets to be literally torn off the surface waves. **Figure 1** shows the two main spray generation pathways and mechanisms originally described in the work of Andreas et al. (1995), Resch et al. (1986), Blanchard & Syzdek (1988), and MacIntyre (1972).

### 2.1. Size Conventions

The field of ocean spray and marine aerosol physics and dynamics is, to this day, fraught with various size conventions that mostly stem from the different mechanisms that lead to spray

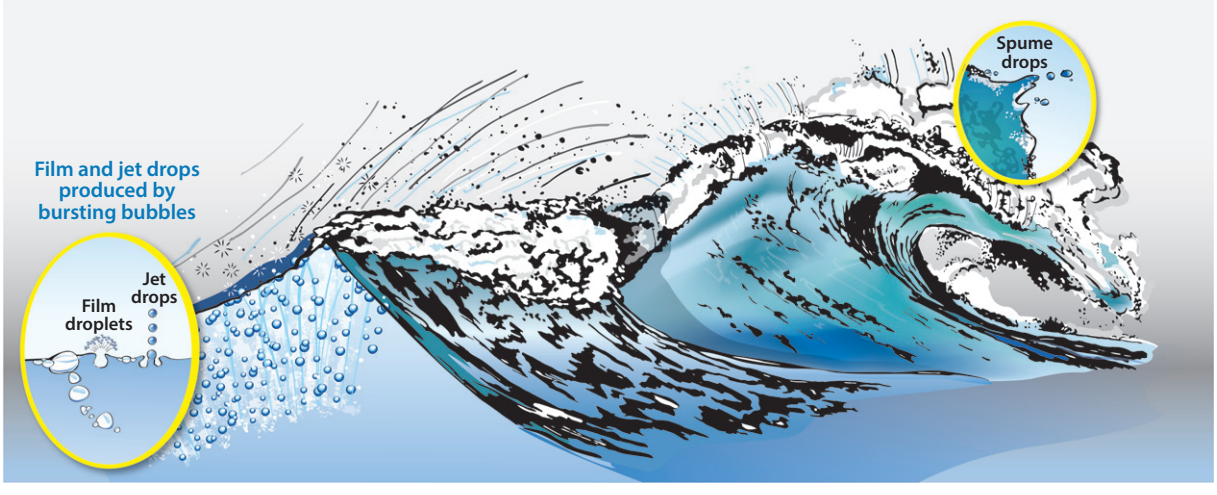


**Figure 1**

The main pathways of sea spray generation. Spray is generated from bubbles bursting at the surface, which create film and jet drops; spume drops are ejected from the breaking wave crest when the wind shear is sufficiently large. Figure adapted from Andreas et al. (1995, figure 1).

formation and from the different dynamic timescales of various spray-mediated processes for the whole range of sea spray sizes. In this review, I favor the use of the drop radius instead of the diameter. As shown below, the range of drop and particle radii spans at least six orders of magnitude, with aqueous particles observed with radii as low as 10 nm (Bigg & Leck 2008) to as large as several millimeters (Anguelova et al. 1999, Veron et al. 2012).

Accordingly, the timescales associated with the various dynamic interactions between the drops and the environment span a comparably large domain. Consequently, specific size conventions are more relevant depending on the droplet size range and the particle processes of interest. For example, large spray droplets ejected from the crest of breaking waves have radii on the order of $O(40)$ μm to several millimeters, and their life span in the atmosphere is on the order of seconds. For these drops, it is practical to use the radius at formation $r_0$ as a relevant size. Conversely, for medium-size drops that stay suspended for minutes to hours, get transported away from the moist atmosphere near the ocean surface, and evaporate substantially, the use of $r_{80}$, the equilibrium radius at an equivalent 80% relative humidity, is preferred. For these droplets, $r_{80}$ is a rather convenient standard because it is typically difficult to measure these drops at formation in the field and also because they adjust to the ambient relative humidity relatively quickly. These medium-size drops are taken here to be in the range 1 μm $< r_{80} <$ 25 μm. For small particles ($r_{80} <$ 1 μm), with an atmospheric residence time of several days, $r_{80}$ can be used if the droplet has not evaporated entirely. Alternatively, for these small particles, $r_d$, which is the volume equivalent radius of the dry (salt) particle left when the drop has evaporated, is also regularly used. The phase transition from a saline liquid drop to a solid particle (efflorescence) occurs when the relative humidity is below ∼50% (Tang et al. 1997). For typical sea spray salinity,

$$r_0 \sim 2r_{80} \sim 4r_d \tag{1}$$

is an adequate rule of thumb. More precise relationships can be found in Fitzgerald (1975).

I adopt here the small, medium, and large sea spray–droplet nomenclature proposed by Lewis & Schwartz (2004, p. 11). These designations are convenient because they follow several properties of the droplets, such as the atmospheric residence time; dynamic behaviors; evaporation times; and, to some extent, the production mechanism. Accordingly, these size ranges offer qualitative and practical size brackets but should not be taken as rigidly defined boundaries. In this review, I also focus on aqueous droplets and thus refer here principally to $r_{80}$ and $r_0$.

## 2.2. Bubble-Generated Spray Droplets

To begin, let us examine the droplets generated by bubble bursting at the surface. When surface waves break, a significant amount of air is entrained into the water column (Thorpe 1992, Melville 1996). The smallest bubbles may dissolve entirely, but a large fraction of the total amount of air entrained, the void fraction, makes it back to the surface layer in the form of bubbles. A typical breaking wave crest in the ocean is thus followed by a turbulent wake capped with a foamy layer, the whitecap (Monahan 1971; Monahan & O'Muircheartaigh 1980, 1986; Bondur & Sharkov 1982; Kleiss & Melville 2011). Thus, the film and jet drops are typically generated behind the breaking wave crest (**Figure 1**). Because of the difficulty of making field measurements close to the surface with sufficient spatial and temporal resolution to observe the film and jet drop generation, the details of their generation mechanisms have necessarily been obtained in the laboratory (Wu 1973, Lai & Shemdin 1974, Cipriano & Blanchard 1981, Resch et al. 1986, Resch & Afeti 1991, Mårtensson et al. 2003, Sellegri et al. 2006, Keene et al. 2007, Fuentes et al. 2010).

**2.2.1 Film drops.** After a bubble reaches the ocean surface, its upper (air-side) surface protrudes from the air-sea interface. This bubble cap drains, thins, and eventually shatters in a spectacular event that projects film drops into the atmosphere (Spiel 1998). Resch et al. (1986) and recently Lhuissier & Villermaux (2012) provided remarkable photographs of this type of event, which lasts only $O(10)$ μs. Overall, film drops have been reported with radii from 10 nm (Mårtensson et al. 2003, Sellegri et al. 2006) to several 100 μm (Afeti & Resch 1990, Spiel 1998), but most are less than 1 μm in radius (Gong et al. 1997, Mårtensson et al. 2003, de Leeuw et al. 2011). As a rule of thumb, I consider here that film drops have $r_{80}$ between 0.01 μm and 1–2 μm.

The number of film drops generated by a bursting bubble increases with increasing bubble radius and can reach several hundreds of droplets for bubbles with radii of $O(3–5)$ mm (Blanchard 1963, Spiel 1998, Wu 2001). Bubbles less than 0.5–1 mm in radius, however, probably do not produce film drops (Blanchard 1963, Resch & Afeti 1991, Wu 1994, Andreas 2002). Moreover, because large bubbles in the ocean surface layers are less numerous than small ones (Deane & Stokes 2002), a peak in the distribution of film drops can be expected. Evidence suggests that the film drop distribution has a relatively broad peak, approximately situated around $r_{80}$ in the range 0.1–0.5 μm (O'Dowd & de Leeuw 2007, Fuentes et al. 2010). Finally, the ejection velocity of the film drops can reach 20 to 30 m $s^{-1}$ owing to the large accelerations involved in the rupture of the film cap (Spiel 1998).

Bird et al. (2010) and Lhuissier & Villermaux (2012) have presented recent advances in understanding the draining of the bubble cap and the subsequent formation of film drops, although these results might prove difficult to apply to bubbles in seawater. Indeed, bubbles at sea will collect hydrophobic substances while rising to the surface, and these substances will eventually collect in the bubble cap. Furthermore, in the field, the bubble cap will accumulate natural surfactants and other biochemical compounds (Bigg & Leck 2008, Vignati et al. 2010, Modini et al. 2013). These chemical species will eventually be ejected with the film drops (Blanchard 1964, Keene et al. 2007). Consequently, the composition of film drops is usually more representative of the oceanic surface film rather than of the bulk of the fluid (Blanchard 1964).

Equally important is that the generation mechanism of these drops is affected by the chemical composition and surfactant concentration in the bubble cap (Sellegri et al. 2006, Modini et al. 2013). However, the influence of surfactant, organic matter, and inorganic chemicals on the generation of film droplets is still poorly understood. Once airborne, these film drops will also take part in various chemical reactions in the atmosphere. The implications and role of organic and inorganic chemicals of marine origins on the global aerosol chemical cycle remain to be fully explored. Still, most atmospheric sea salt aerosols that are less than 1 μm in diameter likely originate from film droplets (de Leeuw et al. 2011).

**2.2.2. Jet drops.** Once the bubble cap has shattered, the remaining cavity collapses violently, and a vertical jet forms (MacIntyre 1972). The jet then fragments into several droplets that are ejected into the air several millimeters above the surface (Spiel 1997). Kientsler et al. (1954) offered striking photographs of the creation of jet drops following the bubble bursting event. These photographs allowed them to determine that the ejected drop radii were approximately one-tenth of the bubble radius. The work of Blanchard (1989) and Spiel (1994a,b) showed a departure from this rule, especially for large bubble sizes for which a bubble of radius $r_b = 1{,}000$ μm would produce drops of radii 150 μm, for example. Wu (2002) concluded that drops are likely to scale from 0.13 to 0.15 times the parent bubble size. Spiel (1994a, 1997) and Wu (2002) further differentiated between the top drop and lower drops when multiple droplets are generated.

Contrary to the case of film drops, the number of jet drops produced diminishes with increasing bubble radius. Bubbles with radii larger than approximately 1.5 mm do not appear to generate jet drops (Wu 2002). Up to five to six jet drops are observed for bubble radii of approximately $r_b = 300$ μm (Spiel 1997, Wu 2002). Considering that bubbles with radii less than approximately 20 μm dissolve in the water column, jet drops consequently have radii in the range 2–200 μm. In addition, the ocean bubble spectrum decays quickly with increasing bubble radius (Deane & Stokes 2002); thus, not only are bubbles smaller than 1 mm more frequently found in the field, they also tend to generate more jet drops. Thus, I consider here that jet drops have formation radii $r_0$ in the range 2–100 μm, or $r_{80}$ in the range 1–50 μm (Andreas 2002, Lewis & Schwartz 2004, de Leeuw et al. 2011). The peak of the jet drop distribution is believed to be approximately $r_0 = 10$ μm (Wu 1992, Andreas 2002, Hoppel et al. 2002).

The collapse of the bubble is a rapid and energetic process that leads to a rapid acceleration of the jet (MacIntyre 1972). The resulting drop ejection speeds can reach 8 m $s^{-1}$ for the smallest top drop to 0.3 m $s^{-1}$ for the largest of secondary drops (Spiel 1995, 1997). This results in ejection heights on the order of 10–20 cm for large jet drops (Blanchard 1989).

Similar to film drops, although perhaps to a lesser extent (Facchini et al. 2008), jet drops have been observed to have a composition that can differ significantly from that of bulk ocean water (Bigg & Leck 2008). For example, Blanchard & Syzdek (1972) showed significantly increased bacteria concentration in jet drops. This enhanced concentration in bacteria, as well as in viruses (Aller et al. 2005) and toxins, can lead to adverse health risks, especially in coastal areas where sea spray is generated in the surf zone and can be transported inland (see Fleming et al. 2005 for a short overview).

## 2.3. Spume Drops

Spume droplets are formed when the wind stress is sufficiently large to tear off water from the crest of the waves (**Figure 1**). A wind speed higher than approximately 7–11 m $s^{-1}$ is typically necessary to generate spume droplets (Andreas et al. 1995, Andreas 2002). After being ejected from the breaking wave crest, the droplets are then swept downwind of the crest (**Figure 1**). I note here that in coastal areas, the phase speed of the wave may be sufficient to provide the necessary surface shear to generate spume drops in the absence of high mean wind speed. These drops would appear to be swept behind the wave crest and, in the absence of wind, would obviously fall back into the ocean relatively quickly.

Although observations of breaking waves at sea, or in the coastal zone, suggest that spume drops are generated at the crest of breaking waves, we know much less about the spume drop generation mechanism than we do about the generation of film and jet drops. Koga (1981) was perhaps one of the first to observe the generation of spume drops. He detected drops as large as $r_0 = 400$ μm and measured their velocity in the airflow. Most subsequent studies assumed that spume droplets have radii in the range $r_0 = 10$–500 μm with a peak centered at $r_0 = 100$ μm (Andreas 1992, 1998, 2002; Smith et al. 1993; Wu 1993; Fairall et al. 1994; Andreas et al. 2010). Fairall et al. (2009) measured drops up to $r_0 = 700$ μm; Veron et al. (2012) measured a significant number of spume drops with radii as large as $r_0 = 2$ mm in the laboratory. Spume droplets with radii as large as $r_0 = 6$ mm have also been observed in the laboratory (Anguelova et al. 1999). These extremely large spume drops are likely to fall back within a fraction of a second, except in the most extreme winds. Whereas it was previously thought that spume drops larger than approximately $r_0 = 500$ μm would have no appreciable impact on the heat, moisture, and momentum flux (and certainly

would not take part in the aerosol cycle), their influence on the air-sea momentum balance could be substantial if they happen to be generated in significant numbers.

The details of the generation mechanism of the spume droplets were not re-examined until Mueller & Veron (2009b) postulated that drops were generated from the turbulent fragmentation of large globules resulting from a transverse instability of a breaking wave crest (Marmottant & Villermaux 2004). Veron et al.'s (2012) recent observations partially confirmed this phenomenon but also revealed that the bag breakup (Villermaux 2007) of small lenticular canopies of water inflated by the wind is a potential spume droplet generation mechanism. This latter result remains to be confirmed. Andreas et al. (2010) inferred that the initial ejection velocity of spume droplets should scale with the value of the wind speed at the wave crest, but there are no available data to date to confirm this assumption.

### 2.4. Other Spray Generation Mechanisms

Mechanisms other than bubble bursting and the tearing off of spume drops from the ocean surface also exist, although they are believed to be much less efficient. One such mechanism generates so-called splash drops (Andreas 2002), which are generated when a plunging wave impinges on the surface and bounces back in the form of a splash-up (Kiger & Duncan 2012). Not unlike the drops generated by the free fall of a plunging crest, splash drops are likely to fall back into the ocean very quickly in the absence of wind. In the presence of wind, they could be further fragmented and transported downwind. Although these drops might be roughly included in the spume population, it might be relevant to discriminate among the different generation mechanisms in the hopes of accurately parameterizing drop ejection sizes and velocities based on wave parameters (Mueller & Veron 2009b). Also, spume droplets are created at the high wind crest of waves, while splash droplets are created in the sheltered lee of the crest (at lower height). In fact, future attempts to develop physically based parameterizations of spray generation might need to differentiate between (large) drops that are ejected from the surface, be it by splash or direct tearing, and the daughter droplets that result from the breakup of the initial drops (Pilch & Erdman 1987).

Another mechanism that is, to the best of my knowledge, not yet studied is the sea spray generation following the impact of raindrops on the surface. There is a large body of literature on the impact of liquid drops on liquid surfaces, particularly in the engineering literature, but there are comparatively few environmental studies. These are limited to rain effects on wave damping and underwater sound generation (Prosperetti & Oguz 1993). It is known that rainfall entrains bubbles and generates cavities that also collapse, giving rise to several jet drops, but I am not aware of any estimates of the possible implications of rain on the generation of sea spray.

## 3. SPRAY DROPLETS IN THE NEAR-SURFACE AIRFLOW

Once a water droplet is ejected from the surface, it will interact with the airflow, exchanging momentum, heat, and moisture with the surrounding air (ignoring chemical reactions). Below, I separately summarize the dynamics and thermodynamics of sea spray droplets in the airflow above the sea surface.

### 3.1. Droplet Motion

To be able to describe the dispersion and transport of spray droplets and understand the influence of the airflow and turbulence on spray processes, we need to examine the motion of single drops.

In an unsteady airflow, the equation of motion of small spherical rigid particles of radius $r$ and constant density $\rho_p$ is given by (Maxey & Riley 1983)

$Re_p$: particle Reynolds number

**Stokes relaxation time ($\tau_p$):** time required for a particle to reach 63% of its final velocity when exposed to an impulse transient forcing

$$\begin{aligned}\left(\frac{4}{3}\pi r^3\rho_p\right)\frac{\mathrm{d}\mathbf{v}}{\mathrm{d}t} &= 6\pi r\mu(\mathbf{u}-\mathbf{v})\\ &+\frac{4}{3}\pi r^3\rho_p\mathbf{g}\\ &+\left(\frac{4}{3}\pi r^3\rho\right)\left(\frac{D\mathbf{u}}{Dt}-\mathbf{g}\right)\\ &+\frac{1}{2}\left(\frac{4}{3}\pi r^3\rho\right)\left(\frac{D\mathbf{u}}{Dt}-\frac{\mathrm{d}\mathbf{v}}{\mathrm{d}t}\right)\\ &+6r^2\sqrt{\pi\rho\mu}\int_0^t\left(\frac{\mathrm{d}\mathbf{u}}{\mathrm{d}t'}-\frac{\mathrm{d}\mathbf{v}}{\mathrm{d}t'}\right)\frac{\mathrm{d}t'}{\sqrt{t-t'}}.\end{aligned} \tag{2}$$

It is presented here without the effects of flow curvature (Faxen effects). The velocity vector of the air at the location of the particle is given by $\mathbf{u}$ and the velocity of the particle is denoted by $\mathbf{v}$. The gravitational acceleration vector is $\mathbf{g}$. The density and dynamic viscosity of the air are $\rho$ and $\mu$, respectively. The equation above is valid for small particle Reynolds numbers, $Re_p = (2r|\mathbf{v}_s|)/\nu$, where $\nu$ is the kinematic viscosity of the air, and $\mathbf{v}_s = \mathbf{v} - \mathbf{u}$, the so-called slip velocity, is the difference between the drop velocity and the surrounding air velocity.

On the right-hand side of Equation 2, the first term is the steady viscous drag, $\mathbf{F_D}$, on the particle; the second term is the gravity term; the third term accounts for forces from the fluid on the droplets and includes pressure gradient and viscous forces; the fourth term is the so-called added mass term, which represents the forces from the acceleration of the surrounding fluid; and the last term is the Basset history term, which accounts for past relative acceleration in an unsteady flow and can be related to the development of the boundary layer around the drop or the diffusion of vorticity from the accelerating drop. I note that the formulation above also neglects lift effects from velocity gradients in the air (Saffman lift) and effects from the rotation of the drop (Magnus effect). Forces arising from temperature gradients in the air, Brownian motion, and the motion inside the drop have also been neglected (Crowe et al. 1998).

I use here the following material derivatives:

$$\frac{\mathrm{d}}{\mathrm{d}t} = \frac{\partial}{\partial t} + \mathbf{v}\cdot\nabla \quad \text{and} \quad \frac{D}{Dt} = \frac{\partial}{\partial t} + \mathbf{u}\cdot\nabla, \tag{3}$$

which are equivalent at low $Re_p$ and are frequently interchanged in the added mass term of Equation 2 (Auton et al. 1988, Magnaudet et al. 1995). Collecting terms and rewriting Equation 2 for the drop velocity yield

$$\begin{aligned}\left(1+\frac{\rho}{2\rho_p}\right)\frac{\mathrm{d}\mathbf{v}}{\mathrm{d}t} &= \frac{1}{\tau_p}(\mathbf{u}-\mathbf{v})\\ &+\left(1-\frac{\rho}{\rho_p}\right)g\\ &+\frac{3}{2}\left(\frac{\rho}{\rho_p}\right)\frac{D\mathbf{u}}{Dt}\\ &+\left(\frac{9}{2\pi}\right)^{\frac{1}{2}}\left(\frac{\rho}{\rho_p}\right)^{\frac{1}{2}}\left(\frac{1}{\tau_p}\right)^{\frac{1}{2}}\int_0^t\left(\frac{\mathrm{d}\mathbf{u}}{\mathrm{d}t'}-\frac{\mathrm{d}\mathbf{v}}{\mathrm{d}t'}\right)\frac{\mathrm{d}t'}{\sqrt{t-t'}},\end{aligned} \tag{4}$$

where $\tau_p = \left(2r^2\rho_p\right)/(9\mu)$ is the Stokes relaxation time for the particle (i.e., the particle response time to the Stokes viscous drag force).

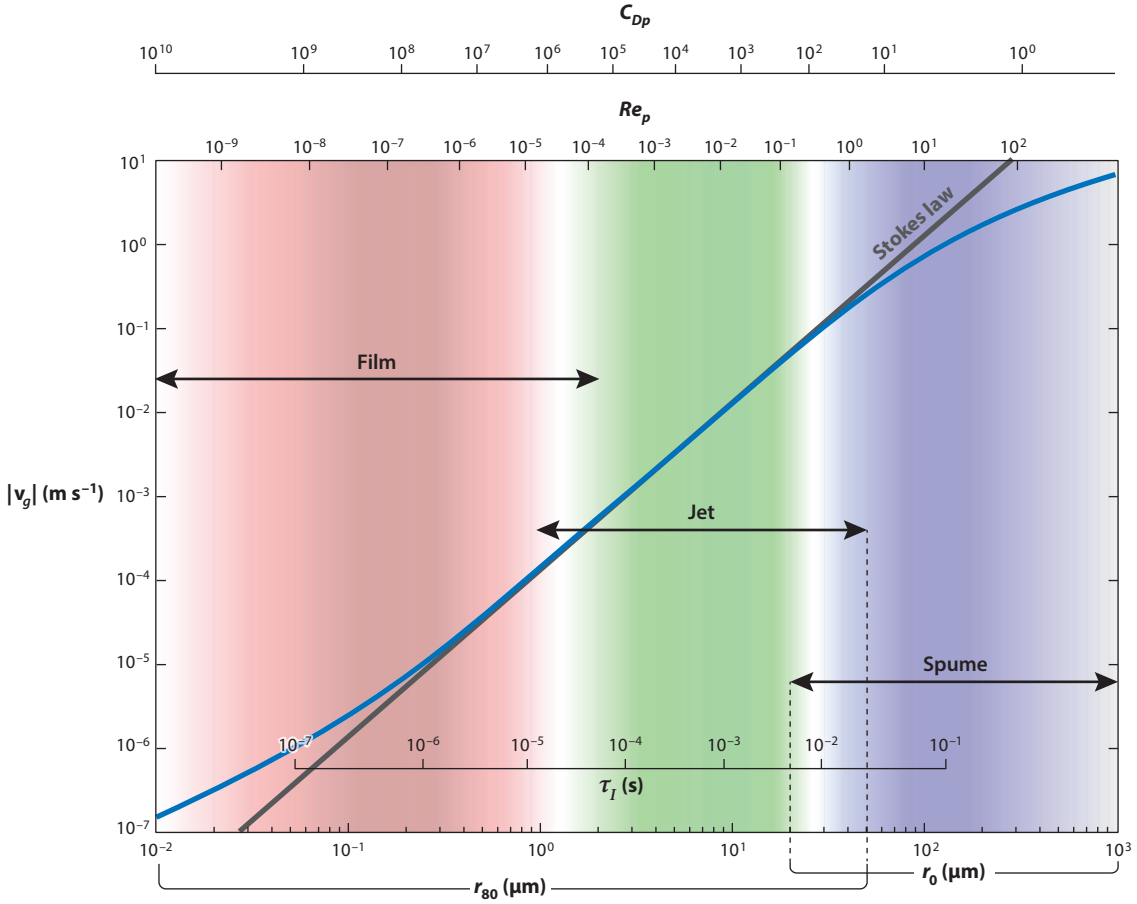


**Figure 2**

Terminal fall velocity of a water droplet in quiescent air at ambient temperature and pressure. The gray line shows the Stokes solution. Additional axes shown are the particle Reynolds number, $Re_p$, and drag coefficient, $C_{Dp}$, as well as the particle inertial relaxation time. Also shown is the size range for the film, jet, and spume drops.

In addition, if the flow is steady and uniform (Stokes flow), Equation 4 further reduces to

$$\left(1+\frac{\rho}{2\rho_p}\right)\frac{\mathrm{d}\mathbf{v}}{\mathrm{d}t}=\frac{1}{\tau_p}(\mathbf{u}-\mathbf{v})+\left(1-\frac{\rho}{\rho_p}\right)\mathbf{g}. \tag{5}$$

The Stokes terminal fall velocity can then be readily estimated as the sum of a gravitational component, $\mathbf{v}_g$, and an advective component, $\mathbf{u}$:

$$\begin{aligned}\mathbf{v}_t &= \tau_p\left(1-\frac{\rho}{\rho_p}\right)\mathbf{g}+\mathbf{u}\\ &= \mathbf{v}_g+\mathbf{u}.\end{aligned} \tag{6}$$

**Figure 2** shows $|\mathbf{v}_g|$, the Stokes terminal velocity given by Equation 6 for a water droplet in quiescent air at ambient pressure and temperature.

Alternatively, the viscous drag force $\mathbf{F_D}$ can be described using the classical formulation in which the drag force on the particle is related to its cross section, $A=\pi r^2$, a quadratic function

of the particle slip velocity, $\mathbf{v}_s$, and a dimensionless drag coefficient, $C_{Dp}$:

$$\mathbf{F_D} = \frac{1}{2}\rho C_{Dp} A(\mathbf{u} - \mathbf{v})|\mathbf{u} - \mathbf{v}|. \tag{7}$$

In Stokes flow with $Re_p < 1$, the viscous drag is $\mathbf{F_D} = 6\pi r\mu(\mathbf{u} - \mathbf{v})$, and the drag coefficient is thus given by $C_{Dp} = 24/Re_p$.

For larger Reynolds numbers, the flow around the particle becomes turbulent, and the drag forces are typically parameterized through empirical corrections to the drag coefficient. For large Reynolds numbers, a widely used relationship is given by Clift & Gauvin (1970), who proposed

$$C_{Dp} = \frac{24}{Re_p} C_f \quad \text{with} \quad C_f = \left(1 + 0.15 Re_p^{0.687} + \frac{0.0175 Re_p}{1 + 4.25 \times 10^4 Re_p^{-1.16}}\right), \tag{8}$$

valid for solid spherical particles with Reynolds numbers up to $O(10^5)$. This correction leads to a departure from Stokes flow, which is reflected in the terminal velocity at drop radii more than approximately 30 μm. In **Figure 2**, at $Re_p > 1$, the particle terminal velocity is significantly reduced when compared to the Stokes flow solution.

For water drops with $r > O(5)$ mm, the spherical assumption breaks down, and one needs to account for the deformation of the drops. In steady flow, this leads to a maximum terminal drop velocity of approximately 9 m $s^{-1}$ for rain drops, and a maximum stable rain drop radius on the order of 3–5 mm, beyond which fragmentation occurs (Villermaux & Bossa 2009). For the case of large spray droplets ejected from breaking wave fronts, these droplets may not attain terminal velocity before falling back into the ocean, and it is likely that spume droplets significantly larger than $r_0 \sim O(3–5)$ mm may exist, at least temporarily (Veron et al. 2012). Conversely, large spume droplets will also fragment under the effect of the shearing force provided by the ambient turbulence in the airflow, especially at high wind speeds, without having necessarily reached terminal velocity (Mueller & Veron 2009b).

For drop radii less than 0.3–0.4 μm, one needs to account for noncontinuum effects. Indeed, at these scales, the drop radii approach the molecular mean free path in air, $\lambda = 68$ nm (at ambient pressure and temperature). For Knudsen numbers, $Kn = \lambda/r$, larger than $10^{-2}$, the continuum assumption starts to break down. At boundaries, the no-slip velocity assumption does not strictly apply starting at $Kn > 10^{-3}$. For the range of radii relevant to sea spray, the drag law can be corrected without requiring full kinetic theory, using

$$C_{Dp} = \frac{24}{Re_p C_c}, \quad \text{with} \quad C_c = 1 + Kn(1.257 + 0.4e^{\frac{-1.1}{Kn}}). \tag{9}$$

The Cunningham slip factor correction, $C_c$, leads to a reduction of the Stokes viscous drag (and an increase in the expected terminal velocity) (Cunningham 1910, Davies 1945). In practice, at these scales, the turbulent motion in the air will dominate, and the drop will be subjected to the velocity fluctuation in the air. For the study of sea spray, the concept of terminal fall velocity is nearly irrelevant at these scales. For the smallest spray droplets in a turbulent flow, the average settling velocity, the so-called deposition velocity $\mathbf{V}_d$ is used instead (Slinn & Slinn 1980). It typically accounts for impaction processes (i.e., the effects of the drop's inertia in a turbulent fluid) and molecular diffusion.

In turbulent flows, one can examine the behavior of a particle relative to that of the fluid using the Stokes number $St = \tau_p/\tau_k$, the ratio between the particle response time and a timescale of the turbulence. The latter is generally taken to be the Kolmogorov timescale. Droplets with $St \ll 1$ respond instantaneously to the airflow fluctuations, down to the smallest turbulent eddies. Thus, the drops will diffuse in such turbulent flows as passive scalars would. For $St \gg 1$, the drop's

inertia is so large that the particle is essentially insensitive to the turbulence. For these drops, the dynamics are nearly ballistic. Particles with $St \sim 1$ will be affected only by airflow turbulent fluctuations with frequencies lower than $1/\tau_k$. Accordingly, these particles tend to be centrifuged to the peripheries of turbulent eddies and accumulate in regions of low vorticity and high strain rates. Hence, the diffusivity associated with these particles will be significantly reduced (Kepert et al. 1999). Other timescales can be chosen from the relevant length and velocity scales and according to the flow conditions at hand. In the ABL, a relevant length scale is $\kappa z$, with $\kappa \approx 0.4$ the von Kármán constant and $z$ the height above the mean water level. The velocity scale is usually chosen as the friction velocity $u_*$. In this case, the Stokes number is $St_* = (\tau_p u_*)/(\kappa z) \approx (|\mathbf{v}_g| u_*)/(g\kappa z)$. Also, we find that $St_* = St Re_*^{-\frac{1}{2}}$, where the Reynolds number $Re_* = (\kappa u_* z)/\nu$ can be viewed as the ratio of the eddy viscosity $\kappa u_* z$ to the molecular viscosity $\nu$. Andreas et al. (2010) used an alternate definition of the Stokes number. In their derivation of the deposition velocity, they defined $St^+ = (\tau_p u_*^2)/\nu = St Re_*^{1/2} = \tau_p^+$, which can be thought of as simply the Stokes timescale expressed in wall units.

**Stokes number ($St$):** measures the ratio of the particle inertial relaxation time to the timescale characteristic of the turbulent flow

Note here that when the Cunningham and large $Re_p$ number corrections of Equations 8 and 9 are applied to the Stokes viscous drag, the Stokes timescale is in turn corrected, leading to a more general expression for the inertial timescale:

$$\tau_I = \tau_p \frac{C_c}{C_f}. \tag{10}$$

Substituting $\tau_I$ for $\tau_p$ in Equation 6 gives the particle terminal velocity plotted in **Figure 2**. The inertial relaxation time $\tau_I$ can also be used in place of $\tau_p$ to estimate $St$.

From **Figure 2**, it would appear that the Stokes flow applies to a relatively small fraction of the range of radii relevant to sea spray. In fact, although it is tempting to neglect most terms in Equation 4 under the precept that $\rho/\rho_p \ll 1$ for sea spray, inhomogeneities and unsteadiness associated with the turbulent airflow in the ABL can be such that the fluid and particle accelerations $D\mathbf{u}/Dt$, $\mathrm{d}\mathbf{u}/\mathrm{d}t$, and $\mathrm{d}\mathbf{v}/\mathrm{d}t$ may be of the same order of magnitude as $\mathbf{g}$, and may be many times $\mathbf{g}$ when film and jet drops are generated. This would then require the use of Equation 4 without simplifications. Furthermore, Equation 4 may in fact need to be complemented and to incorporate flow curvature effects (Faxen effects), which will become important close to the surface. Unfortunately, at high particle Reynolds numbers, corrections to all the terms in Equation 4, except for the viscous drag term, are not satisfactory and may lead to errors yet to be quantified (Crowe et al. 1998).

### 3.2. Dynamic Effects on the Atmospheric Boundary Layer

From the discussion above, it is evident that the transport of sea spray in the ABL is not yet a fully resolved problem. Current work revolves around the potential effects of the spume on the air-sea momentum flux. In particular, spray effects have been offered as a potential candidate to explain the observed reduction of the air-sea momentum flux (i.e., the saturation of the air-sea drag coefficient) in hurricane-force winds (Powell et al. 2003, Donelan et al. 2004, Bell et al. 2012). Several theoretical and numerical studies have indeed shown, through a variety of effects, that the presence of spray in significant quantities in the ABL does reproduce the observed saturation of the drag coefficient in high winds (Bye & Jenkins 2006, Liu et al. 2012).

One avenue of investigation focuses on the role of the spray in the direct exchange of momentum with the airflow and the redistribution of this momentum throughout the ABL by acceleration and deceleration of the drops during their flight (Andreas 2004, Makin 2005, Richter & Sullivan 2013, Mueller & Veron 2014a,b). Ultimately, the net momentum lost or gained by a single drop

that returns to the ocean is

$$\Delta \mathbf{p}_{\mathrm{sp}}(r) = \left(\frac{4}{3}\pi\right)\left[(r^3\rho_p\mathbf{v})_{t=t_f} - (r^3\rho_p\mathbf{v})_{t=0}\right], \tag{11}$$

where $t_f$ is total flight time of the droplet.

**Sea spray generation function (SSGF):** the size-dependent number of droplets generated per unit area of ocean surface, per unit time

As shown below, significant evaporation can take place during a drop's journey through the ABL; the loss of water mass along the way leads to a considerable increase in the drop salinity with a substantial effect on the drop density. The aggregated spray fluxes are discussed in Section 5; for now, it suffices to say that the spray effect on the momentum flux from the small (light) film and jet drops will vastly depend on their number concentration or, perhaps more importantly, the number of drops injected into the airflow, per unit area of ocean surface, per unit time [i.e., a drop flux function or sea spray generation function (SSGF)]. The spume effects suffer from a poorly understood generation process and consequent errors in estimating the initial ejection velocity $\mathbf{v}(t = 0)$. In addition, it can be difficult to estimate the spume drop flight time $t_f$ because of the lack of knowledge of the initial velocity conditions. Nevertheless, order of magnitude estimates can be obtained using $\mathbf{v}(t_f) \sim \mathbf{v}_g$ and $t_f = h_0/|\mathbf{v}_g|$, where $h_0$ is taken to scale with the wave height (Andreas 1992), the height at which these drops are injected into the airflow.

Other avenues of investigation include the possible spray effects on the structure of the turbulence itself (Barenblatt et al. 2005, Rastigejev et al. 2011). Because of the change of the turbulent kinetic energy and buoyant production when the droplets evaporate and alter the stability of the boundary layer, modifications of the Monin-Obukhov similarity theory have been considered (Kudryavtsev 2006, Bao et al. 2011, Bianco et al. 2011, Kudryavtsev & Makin 2011). Rastigejev et al. (2011) showed that these two approaches give similar results, both demonstrating a reduction of the air-sea drag coefficient in the presence of sea spray. I note here that the effects of spray on the air-sea momentum flux are an active area of research and remain a debated and disputed issue; no consensus has yet emerged. Nevertheless, whether because of the change in drop density (momentum) or the flux of water vapor moisture to the atmosphere, it is clear that the thermodynamics of the drops also need to be carefully considered.

### 3.3. Droplet Temperature

For saline drop thermodynamics (i.e., the thermal and evaporation response of the droplet to its environment), I summarize here the work of Andreas (1989), who extended the work of Pruppacher & Klett (1978) on the evolution of aqueous drops to saline sea spray droplets. The evolution of a droplet's size and temperature as it traverses the turbulent ABL can thus be evaluated. Following Andreas (1989), the temporal evolution of the radius of a saline (NaCl) water droplet in air is

$$\frac{dr}{dt} = \frac{f_w D'_w M_w e_s(T_a)}{\rho_p r R T_a} \times \left[Q_{\mathrm{RH}} - \frac{1}{1+\delta}\exp\left(\frac{L_v M_w}{R T_a}\frac{\delta}{1+\delta} + \frac{2 M_w \Gamma_p}{R T_a \rho_w r(1+\delta)} - \frac{I\Phi_s m_s (M_w/M_s)}{(4\pi r^3\rho_p/3) - m_s}\right)\right], \tag{12}$$

where $Q_{\mathrm{RH}}$ is the fractional relative humidity; $\rho_w$ is the pure water density; $R$ is the universal gas constant; $M_w$ and $M_s$ are the molecular weights of water and salt, respectively; $e_s(T_a)$ is the saturation vapor pressure at the air temperature $T_a$; $L_v$ is the latent heat of vaporization; $\Gamma_p$ is the surface tension of a flat surface with the same temperature and salinity as the drop; $m_s$ is the mass of salt in the droplet; $I$ is the number of ions salt dissociates into ($I = 2$); $\Phi_s$ is the osmotic coefficient; and $\delta = T_p/T_a - 1$.

In Equation 12, the term between square brackets simply represents the difference between the ambient humidity $Q_{\mathrm{RH}}$ surrounding the droplet and the humidity at the surface of the drop.

This latter humidity results from three distinct effects that are reflected in the three terms inside the exponential function. The first term accounts for the droplet temperature, which differs from the ambient air temperature. The second term reflects the curvature and surface tension effects. The last term accounts for salinity effects in the spray droplets. Note that the evaporation rate is increased for small droplets and is reduced by salinity (Andreas 1989).

The temporal evolution of the droplet temperature $T_p$ is

$$\frac{\mathrm{d}}{\mathrm{d}t}(T_p - T_a) = \frac{3}{r^2 \rho_p c_{ps}}(f_h k'_a (T_a - T_p) + f_w L_v D'_w(\rho q - q_p)). \tag{13}$$

where $T_p$ is assumed uniform inside the drop. Here, $c_{ps}$ is the specific heat of salty water; $q$ is the specific humidity for moist air such that $\rho q$ is the ambient water vapor density. The water vapor density on the droplet surface is

$$q_p = \frac{M_w e_s(T_p)}{R T_p} \exp\left(\frac{2 M_w \Gamma_p}{R T_a \rho_w r(1+\delta)} - \frac{I \Phi_s m_s (M_w/M_s)}{(4\pi r^3 \rho_p/3) - m_s}\right) \tag{14}$$

and includes, as above, the effects of curvature, surface tension, and salinity. The modified diffusivity for water vapor, $D'_w$, and the modified thermal conductivity of air, $k'_a$, include noncontinuum effects and are

$$D'_w = \frac{\epsilon}{\dfrac{r}{r+\Delta_w} + \dfrac{\epsilon}{r\alpha_c}\left(\dfrac{2\pi M_w}{R T_a}\right)^{1/2}}, \tag{15}$$

$$k'_a = \frac{k_a}{\dfrac{r}{r+\Delta_T} + \dfrac{k_a}{r\alpha_T \rho_{ad} c_{pd}}\left(\dfrac{2\pi M_a}{R T_a}\right)^{1/2}}, \tag{16}$$

where $\epsilon$ and $k_a$ are the molecular diffusivity for water vapor and the thermal conductivity of air, respectively. $M_a$ is the molecular weight of dry air; $c_{pd}$ and $\rho_{ad}$ are the specific heat and density for dry air, respectively, with constants $\Delta_w = 8 \times 10^{-8}$, $\alpha_c = 0.036$, $\Delta_T = 2.16 \times 10^{-7}$, and $\alpha_T = 0.7$. I also include ventilation coefficients $f_w = f_h = 1 + Re_p^{1/2}/4$, which are corrections to the heat and water vapor diffusivity for large instantaneous particle Reynolds numbers (i.e., $Re_p \gg 1$) (Fairall et al. 1994). The two terms in Equation 13 represent the changes to the drop temperature from the sensible and latent heat flux exchanges. Evidently, Equations 12 and 13 need to be solved simultaneously. Simplifications and approximations were proposed by Andreas (1990, 1995, 2005).

**Figure 3** shows the temporal evolution of a saline droplet, with an initial radius of $r_0 = 100$ μm and an initial salinity of $S = 34$ ppt. At formation, the droplet is at the temperature of the bulk ocean, $T_{p0} = 20$°C in this case. The drop rapidly cools down to a constant evaporation temperature $T_{ev}$, which differs slightly from the wet bulb temperature (Andreas 1995). At this point, the drop has reached thermal equilibrium with the surrounding environment and has thus exchanged sensible heat with the air. In the case shown in **Figure 3**, the evaporation temperature was reached in less than 1 s. During this initial phase, the droplet retains almost all of its water mass. **Figure 3** also shows the time evolution of the droplet's radius. In these conditions, the drop will evaporate and reach an equilibrium radius of $r_{eq} = 47$ μm. This reduction in radius increases the salinity by more than a factor of eight, leading to a non-negligible 15% increase in density. The evaporation process is much slower, the drop will not significantly evaporate before $t = 2$ s, and it will reach $r_{eq}$ at approximately $t = 200$ s. Much of the latent heat flux between the drop and the atmosphere takes place after the sensible heat exchange has ceased and while the drop temperature is at $T_{ev}$, hence the name evaporation temperature. When the rate of evaporation

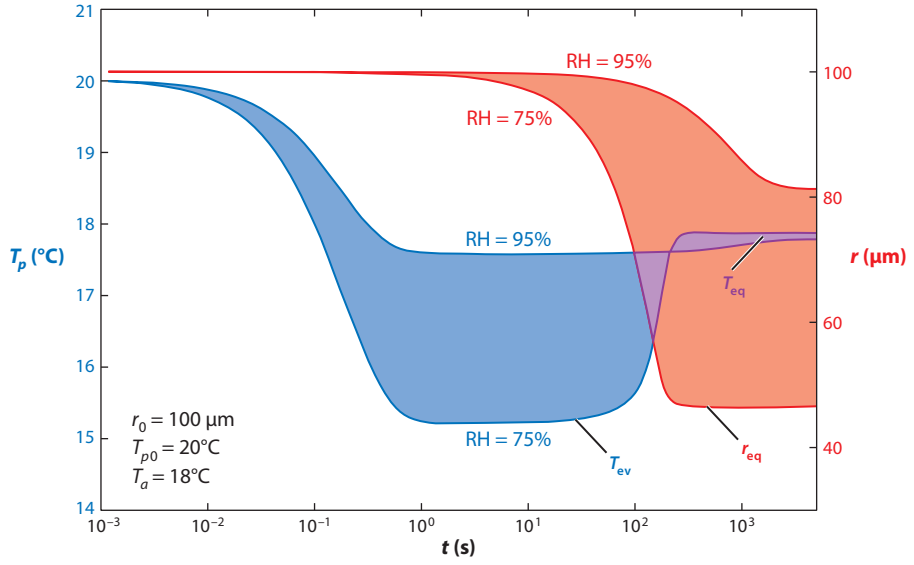


**Figure 3**

Time evolution of a water droplet's temperature (*blue*) and radius (*red*). The droplet is assumed to be in quiescent air at $T_a = 18$°C and standard atmospheric pressure. The drop has an initial radius of $r_0 = 100$ μm and initial temperature of $T_{p0} = 20$°C. The shaded areas show the range of drop temperature and radius for relative humidity (RH) between 75% and 95%.

decreases, the temperature of the drop rises back toward the air temperature and finally stabilizes at an equilibrium temperature, $T_{eq}$, when the radius reaches $r_{eq}$ (Andreas 1995). As a general rule, $T_{ev}$ increases with the relative humidity and $T_a$. $T_{ev}$ also decreases with radius. When the equilibrium radius has been reached, $T_{eq}$ is largely insensitive to the relative humidity (see **Figure 3**) but is proportional to $T_a$. As one would expect, $r_{eq}$ increases with the relative humidity. It also increases weakly with $T_{p0}$ and is largely independent of $T_a$.

From **Figure 3**, it is clear that the sensible and latent heat exchanges between a spray drop and the atmosphere are essentially decoupled. Noting that the initial temperature and radius changes associated with the sensible and latent heat exchanges are roughly exponential, Andreas (1992) proposed that the temperature and radius evolutions could be represented as

$$\begin{aligned} \frac{T_p(t) - T_{ev}}{T_{p0} - T_{ev}} &= e^{-\frac{t}{\tau_T}}, \\ \frac{r(t) - r_{eq}}{r_0 - r_{eq}} &= e^{-\frac{t}{\tau_r}}, \end{aligned} \tag{17}$$

where $\tau_T$ and $\tau_r$ are the relaxation timescales associated with the temperature change (sensible heat flux) and radius change (latent heat flux), respectively, for the evolution of saline droplets. These timescales are functions of ambient conditions (Andreas 1990). The first timescale is the adjustment time for a droplet to reach an initial thermal equilibrium temperature, $T_{ev}$. Depending on the radius and ambient conditions, it spans a range on the order $10^{-7}$–10 s. The second timescale is the time required for the droplet to lose a significant amount of its water mass and is generally on the order of $10^{-4}$–$10^{5}$ s. **Figure 4** shows $\tau_T$ and $\tau_r$, as well as the inertial timescale $\tau_I$. $\tau_T$ decreases weakly with $T_a$. $\tau_r$ also decreases weakly with $T_a$ and increases with relative humidity.

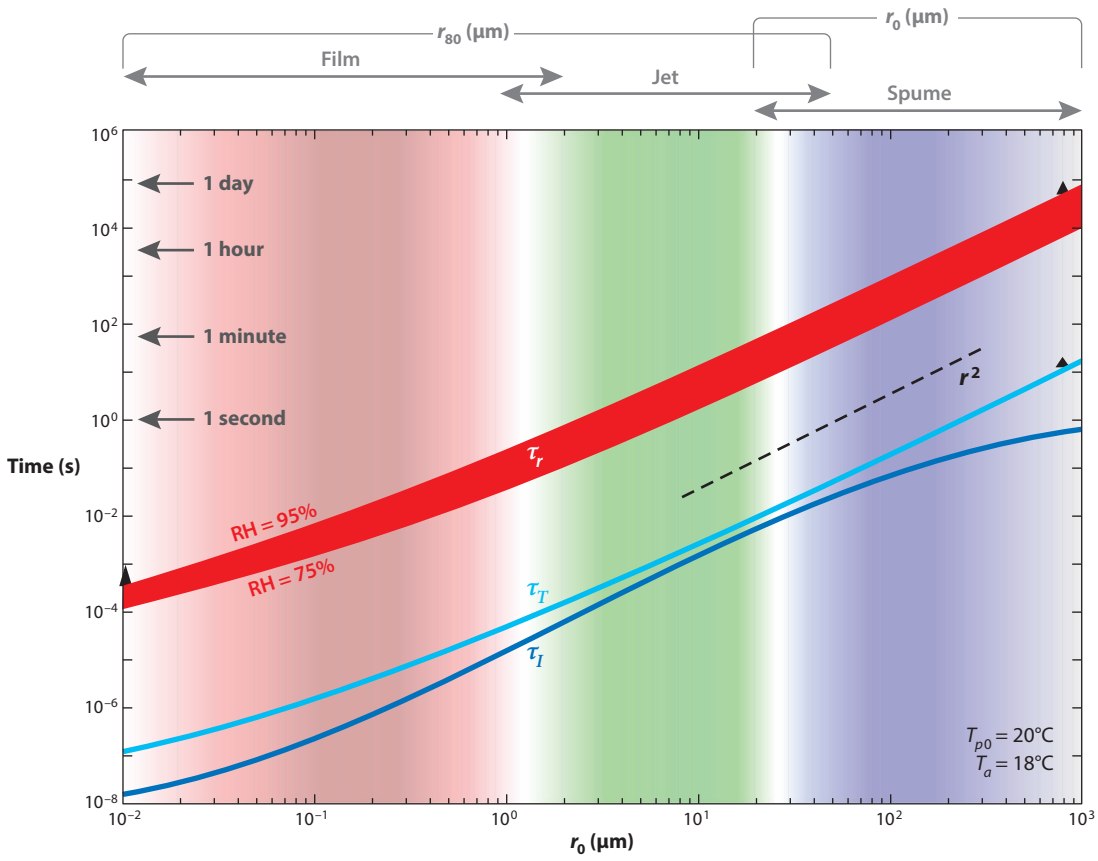


**Figure 4**

Relaxation times for the drop radius (*red*) and temperature (*blue*) as a function of the drop's initial radius. The variation with humidity and air temperature is also shown; the black triangles show where the curves would be displaced for an atmospheric temperature of $T_a = 8$°C. The inertial relaxation time is also plotted for reference.

The timescales $\tau_I$, $\tau_T$, and $\tau_r$ are strong functions of the droplet radius. In fact, all these timescales are proportional to the drop cross section (for $\tau_I$) or the surface area (for $\tau_T$ and $\tau_r$) and thus are proportional to $r^2$, at least for radii $r > 1$ μm, for which noncontinuum effects do not factor in. Small drops are quicker at transferring their sensible and latent heat than are larger ones. For example, in the atmospheric conditions presented above, a droplet with $r_0 = 1$ μm will reach $T_{ev}$ in less than $O(10^{-4})$ s and $r_{eq}$ in less than $O(1)$ s, whereas a droplet with $r_0 = 100$ μm will reach $T_{ev}$ in less than $O(1)$ s and $r_{eq}$ in less than $O(1{,}000)$ s. In other words, as mentioned above, **Figure 4** shows that $\tau_r$ is approximately three orders of magnitude greater than $\tau_T$.

It is informative to think about the drop heat and moisture exchange in terms of timescales because it allows comparison of the flux timescales with the atmospheric residence time of spray droplets, which I denote $t_f$ for flight time. Because small film drops with $r_0 \sim 0.1$–1 μm will remain suspended on the order of several days (Andreas 1990, Lewis & Schwartz 2004), it is thus expected that these droplets will have ample time to reach equilibrium. In fact, a film droplet with $r_0 = 0.1$ μm will reach $T_{ev}$ in approximately $O(10^{-6})$ s and $r_{eq}$ in approximately 0.03 s. This is in part why the use of $r_0$ becomes rapidly irrelevant, and the $r_{80}$ size convention is adopted for these small spray droplets.

Conversely, spume drops with radii on the order of $r_0 \sim 100$ μm may reach thermal equilibrium but are not expected to reach $r_{eq}$ before they fall back into the ocean. For spume droplets then, $T_{eq}$ is not reached either, and $T_{ev}$ is the temperature scale that will measure the amount of the sensible heat exchanged. Furthermore, $T_{ev}$ is a function of both relative humidity and $T_a$, and in the turbulent atmospheric boundary layer near the surface where spume droplets are expected to remain, both temperature and water vapor content fluctuate with the turbulence in the air. Mueller & Veron (2010) demonstrated that the fluctuations in atmospheric water vapor content are most coherent with the fluctuations of drop temperature. The ambient humidity has a tighter relationship with the drop temperature, thereby largely dictating the total sensible heat flux from the spume drop.

### 3.4. Thermodynamic Effects on the Atmospheric Boundary Layer

Similar to the droplet exchanges of momentum with the airflow (Equation 11), sea spray exchanges of heat and moisture with the ABL are of interest, especially in high winds in which spray in the atmosphere is known to be ubiquitous, if only from casual observation. For a drop that falls back into the ocean, such as a spume drop and some film and jet drops, the sensible and latent heat exchanged with the atmosphere can easily be estimated as

$$\begin{aligned} \Delta H_{sp}(r) &= \left(\frac{4}{3}\pi\right) c_{ps}[(r^3 \rho_p T_p)_{t=t_f} - (r^3 \rho_p T_p)_{t=0}], \\ \Delta E_{sp}(r) &= \left(\frac{4}{3}\pi\right) L_v[(r^3 \rho_p)_{t=t_f} - (r^3 \rho_p)_{t=0}], \end{aligned} \tag{18}$$

assuming that neither $c_{ps}$ nor $L_v$ depends strongly on the drop temperature, salinity, or density, which all can change substantially during the drop's flight.

Andreas (1992), for example, utilized the expressions in Equation 17 to estimate the temperature and radius at $t = t_f$ but ignored the effect of drop density changes and differences between $T_{ev}$ and $T_{eq}$, both of which can be significant. In Equation 17, ambient conditions are assumed steady. However, Mueller & Veron (2010) estimated the timescales of the humidity and temperature fluctuations in the near-surface ABL and showed that spray drops will respond to the air turbulence and moisture turbulence. This is especially true for the temperature because $\tau_T$ and $\tau_I$ are of the same order of magnitude.

It becomes clear that the dynamics and thermodynamics of the droplet cannot be solved for completely independently because the thermodynamic response of a droplet will strongly depend on its position and local ambient temperature, as well as the relative humidity and turbulent conditions around the drop. In turn, the trajectory of a droplet strongly depends on its radius and density, both of which are affected by the sensible and latent heat flux from and to the drop. Lagrangian models can account for these effects but are computationally intensive (Mestayer et al. 1996; Edson & Fairall 1994; Mueller & Veron 2009a, 2010), rendering them impractical for routine meteorological applications; it is also extremely difficult to incorporate the feedback effects using a Lagrangian approach. Eulerian models average local spray effects and do incorporate feedback but fail to account for the potential modification of droplet properties during their flight time. Recent studies using Eulerian-Lagrangian approaches in both large-eddy simulation and direct numerical simulation models provide a promising avenue of investigation (Shpund et al. 2011, 2012; Richter & Sullivan 2013, 2014).

Just as Equation 11 gives the momentum exchanged by a single droplet, the expressions in Equation 18 evaluate the sensible and heat fluxes, also from a single drop. To obtain the spray-mediated momentum and heat fluxes, one needs to multiply Equations 11 and 18, respectively, by the SSGF.

## 4. DROP CONCENTRATION AND GENERATION FUNCTIONS

The section above summarizes the dynamics and thermodynamics of individual drops. In the field, however, sea spray droplets are simultaneously generated and subsequently transported over a wide range of radii. As hinted at above, a size-dependent approach is necessary to assess the cumulative impact of sea spray on the environment.

### 4.1. Droplet Size Distribution

The droplet size distribution $n(r)$ is defined such that $n(r)dr$ is the total concentration, the number of drops per unit volume of air ($m^{-3}$), for particle radii in the $[r, r + dr]$ range. Hence, the total number of drops in a unit volume of air is

$$\mathcal{N} = \int_0^\infty n(r)dr. \tag{19}$$

The cumulative concentration

$$N(r_\alpha) = \int_0^{r_\alpha} n(r)dr \tag{20}$$

denotes the number of drops with radii less than $r_\alpha$ in a unit volume of air. It is used to define the drop size distribution as

$$n(r) = \frac{dN(r)}{dr}. \tag{21}$$

Thus, the droplet size distribution $n(r) = dN(r)/dr$ is the number of drops per unit volume of air per $dr$ radius increment. It has units of $m^{-3}\ \mu m^{-1}$, where the radius is typically considered and displayed in micrometers. The droplet size distribution is sometimes referred to as the size-dependent droplet concentration or the droplet number concentration function. Alternatively, it is sometimes more convenient to consider the particle normalized probability density functions $p(r)$ (i.e., the probability of finding a droplet with radius between $r$ and $r + dr$ when a single drop is randomly picked out of a volume of air sufficiently large to contain many droplets):

$$p(r) = \frac{1}{\mathcal{N}}\frac{dN(r)}{dr}. \tag{22}$$

This notation is more widely used in cloud and aerosol physics (Shaw 2003), whereas the sea spray community favors the use of Equation 21.

### 4.2. Conservation of $n(r)$

In general, the size-dependent droplet concentration varies with time, the height above the ocean surface, and perhaps the horizontal location as in the surf zone, or across a coastline or fronts. Hence, the conservation of the size-dependent droplet concentration can be expressed as

$$\frac{\mathrm{d}n(r(t), \mathbf{x}, t)}{\mathrm{d}t} = \nabla \cdot (k_p(r)\nabla n(r(t), \mathbf{x}, t)) + Q_n(r, \mathbf{x}, t), \tag{23}$$

where $k_p(r) = (T_a C_c k_B)/(6\pi r\mu)$ is the size-dependent droplet molecular diffusivity. Here, $T_a$ and $k_B$ are the air absolute temperature and the Boltzmann constant, respectively. $Q_n(r, \mathbf{x}, t)$ is a size-dependent source (or sink) function [i.e., the number of droplets with radius $r$ generated (or removed) per unit time and per unit volume of air per $dr$ radius increment]. Rewriting the total derivative, one obtains

$$\frac{\partial n}{\partial t} = -\nabla \cdot (\mathbf{v}n - k_p\nabla n) + Q_n - \frac{\partial}{\partial r}\left(n\frac{\partial r}{\partial t}\right), \tag{24}$$

where $(r(t), \mathbf{x}, t)$ is omitted to lighten the notation. The last term on the right-hand side of Equation 24 represents a change in the size-dependent concentration $n(r)$ because of droplet evaporation or condensation. Collision, coalescence, and breakup can also be accounted for using so-called continuous or stochastic collection and breakup equations (Pruppacher & Klett 1997, Shaw 2003). However, for typical sea spray conditions, the drop concentration is such that collision and coalescence effects can generally be neglected.

Using standard Reynolds decomposition, in which the drop velocity is decomposed into a mean and a turbulent contribution $\mathbf{v} = \bar{\mathbf{v}} + \mathbf{v}'$, and also decomposing $n$ and $r$, one finds that the averaged conservation equation reduces to

$$\frac{\partial \bar{n}}{\partial t} = -\nabla \cdot \left(\overline{\mathbf{v}' n'} + \bar{\mathbf{v}}\bar{n} - k_p \nabla \bar{n}\right) + \bar{Q}_n - \frac{\partial}{\partial r}\left(\bar{n}\frac{\partial \bar{r}}{\partial t} + \overline{n'\frac{\partial r'}{\partial t}}\right), \tag{25}$$

where the overbars denote ensembles or temporal means, and primes denote deviations. On the right-hand side, the first term is the vertical transport by turbulent diffusion, and the second term denotes the mean vertical droplet velocity. In this form, the last term on the right-hand side is known as the stochastic condensation equation (Shaw 2003). In most sea spray conditions, the relaxation timescale for the drop radius, $\tau_r$, is sufficiently large compared to the timescales in the fluid turbulence for the term $\overline{n'\partial r'/\partial t}$ to be neglected. In this case, one can write Equation 25 more simply as

$$\frac{\mathrm{d}\bar{n}}{\mathrm{d}t} = -\nabla \cdot \left(\overline{\mathbf{v}' n'} - k_p \nabla \bar{n}\right) + \bar{Q}_n \quad \text{or} \quad \frac{D\bar{n}}{Dt} = -\nabla \cdot \left(\overline{\mathbf{v}' n'} + \mathbf{V}_d \bar{n} - k_p \nabla \bar{n}\right) + \bar{Q}_n, \tag{26}$$

where $\mathbf{V}_d = \bar{\mathbf{v}} - \bar{\mathbf{u}}$ is the mean deposition velocity.

In a turbulent flow, in which the drag on a drop is nonlinear and droplets are exposed to turbulent eddies, the mean settling velocity can be somewhat different from the steady gravitational settling velocity of the drops, $\mathbf{v}_g$ (Wang & Maxey 1993). $\mathbf{V}_d$ can also include molecular diffusion effects (Slinn et al. 1978). With the slip velocity $\mathbf{v}_s$, which obviously contains the effects of the drop's inertia, an alternate expression for Equation 26 is (Slinn et al. 1978, Rouault et al. 1991, Kepert et al. 1999)

$$\frac{D\bar{n}}{Dt} = -\nabla \cdot \left(\overline{\mathbf{v}'_s n'} + \mathbf{V}_d \bar{n} + \overline{\mathbf{u}' n'} - k_p \nabla \bar{n}\right) + \bar{Q}_n. \tag{27}$$

Another formulation of Equation 26 was proposed by Meirink (2002), who further decomposed the turbulent deviation ($'$) into a wave-coherent component ($\tilde{}$) and an uncorrelated residual ($''$), such that

$$\frac{D\bar{n}}{Dt} = -\nabla \cdot \left(\overline{\mathbf{v}'' n''} + \overline{\tilde{\mathbf{v}}\tilde{n}} + \mathbf{V}_d \bar{n} - k_p \nabla \bar{n}\right) + \bar{Q}_n. \tag{28}$$

For now, let us incorporate the wave-coherent quantity in the deviation from a mean and express Equation 27 as a simple flux equation (Hoppel et al. 2002):

$$\frac{D\bar{n}}{Dt} = -\nabla \cdot \bar{\mathbf{\Phi}} \tag{29}$$

with

$$\bar{\mathbf{\Phi}} = \left(\overline{\mathbf{v}'_s n'} + \mathbf{V}_d \bar{n} + \overline{\mathbf{u}' n'} - k_p \nabla \bar{n} + \bar{\mathbf{S}}_n\right), \tag{30}$$

where $\bar{Q}_n = -\nabla \cdot \bar{\mathbf{S}}_n$, and $\bar{\mathbf{S}}_n$ is a size-dependent source (or sink) flux function [i.e., the number of droplets with radius $r$ generated (or removed) per unit surface per unit time per d$r$ radius increment]. The size-dependent flux function is generally referred to as the SSGF and is denoted as

$$\bar{\mathbf{S}}_n = \frac{d\mathbf{F}(r)}{dr}. \tag{31}$$

Once again, the SSGF appears as a critical parameter. For one thing, it is necessary to obtain the aggregated spray-mediated fluxes from the individual droplet sensible heat, latent heat, and momentum exchanges given by Equations 11 and 18.

## 4.3. Direct Estimates of the Sea Spray Generation Function

The sea spray generation function $\bar{\mathbf{S}}_n$ is typically very difficult to measure directly, but it can be inferred in a number of ways. Lewis & Schwartz (2004) presented nine different ways to evaluate the SSGF. I present below a short subset of these methods. Let us first look at Equations 29 and 30 in more detail. For open ocean applications, it is practical to consider steady, horizontally homogeneous conditions and look at the vertical transport and distribution of spray. Under these conditions, when projected in the vertical direction ($i = 3$ denoted with a subscript), we obtain $\bar{\Phi}_3 = 0$. Neglecting the particle molecular diffusion $k_p$, one finds that Equation 30 simplifies to

$$\overline{v'_{s3}n'} + \overline{u'_3 n'} - V_d\bar{n} + \bar{S}_{n3} = 0 \text{ or } \overline{v'_3 n'} - V_d\bar{n} + \bar{S}_{n3} = 0, \tag{32}$$

where $V_d = -|\mathbf{V}_d|$ is the vertical downward component of the gravitational settling velocity and is generally positive, and $\bar{S}_{n3} = \int_z^\infty \bar{Q}_n(z)dz$ is the vertical component of the SSGF, or the number of droplets of radius $r$ generated through the (horizontal) sea surface per unit surface per unit time per $dr$ radius increment. $\bar{S}_{n3}$ is usually simply noted as $dF(r)/dr$.

For small film and jet drops for which $V_d$ can be neglected,

$$\bar{S}_{n3} \approx -\overline{v'_3 n'}, \tag{33}$$

and $\bar{S}_{n3}$ can be directly estimated from micrometeorological eddy covariance measurements of $\overline{v'_3 n'}$ (Norris et al. 2012, 2013). This is an effective way to measure the SSGF but requires fast, direct measurements of the size-dependent concentration $n(r)$, which makes it a challenging method.

Alternatively, following Rouault et al. (1991) and Kepert et al. (1999), the turbulent fluxes are parameterized using eddy diffusivity formulations:

$$\begin{aligned} \overline{v'_{s3}n'} &= -K'_{sn}(z)\frac{\partial\bar{n}}{\partial z}, \\ \overline{u'_3 n'} &= -K'_n(z)\frac{\partial\bar{n}}{\partial z}. \end{aligned} \tag{34}$$

And, of course, one obtains

$$\begin{aligned} \overline{v'_3 n'} &= -K'_p(z)\frac{\partial\bar{n}}{\partial z} \\ &= -(K'_n(z) + K'_{sn}(z))\frac{\partial\bar{n}}{\partial z}. \end{aligned} \tag{35}$$

Here, $K'_n(z)$, $K'_{sn}(z)$, and $K'_p(z)$ are the turbulent diffusion coefficients. In particular, we consider $K'_n(z) = (\kappa z u_*)/Sc_{tn}$, with $\kappa u_* z$ the eddy viscosity. The droplet's turbulent Schmidt number, $Sc_{tn}$, for lack of a better parameterization, is taken to be equivalent to that of water vapor (Rouault et al. 1991). Stability effects can also be included in the formulation of $K'_n(z)$, with a similar lack of experimental validation (Goroch et al. 1980, Bao et al. 2011). Equation 32 then reads

$$\begin{aligned} &-(K'_n(z) + K'_{sn}(z))\frac{\partial\bar{n}}{\partial z} - V_d\bar{n} + \bar{S}_{n3} = 0, \\ &-K'_p(z)\frac{\partial\bar{n}}{\partial z} - V_d\bar{n} + \bar{S}_{n3} = 0. \end{aligned} \tag{36}$$

Turbulent diffusion has already been assumed to be much larger than molecular diffusion, but molecular effects can be incorporated in $V_d$ (Slinn et al. 1978). In fact, because the slip velocity is $v'_{s3} = v'_3 - u'_3$, it seems natural to define $K'_{sn}$ as a departure from $K'_n$. Rouault et al. (1991) introduced a slip coefficient $f_s$ and, based on the work of Meek & Jones (1973), presented the following formulation:

$$K'_{sn}(z) = K'_n(z)\left(\frac{1}{1 + C_2\left(\frac{V_d^2}{\overline{u'^2_3}}\right)} - 1\right) \tag{37}$$

‘

$$= K'_n(z)(f_s - 1), \tag{38}$$

where $C_2 \approx 2$ is a constant that is adjusted to match experimental data. As expected, the diffusion of particles with inertia is reduced compared to the diffusion of the fluid turbulence $K'_p(z) = f_s K'_n(z)$. I note here that $V_d^2/\overline{u'^2_3} \sim (St_*/Fr_*)^2$, where $Fr_* = {u_*}^2/(g\kappa z)$ is a Froude number. Equation 36 then yields

$$\frac{\kappa u_* z f_s}{Sc_{tn}}\frac{\partial \bar{n}}{\partial z} + V_d \bar{n} = \bar{S}_{n3}. \tag{39}$$

The SSGF can thus be estimated directly from measurements of the drop concentration average profiles. These direct methods average all quantities over timescales and length scales larger than the specific processes responsible for the generation mechanisms linked to the bubble plumes and wave crests of individual breaking events. The spray generation function is typically very difficult to estimate because of the complicated nature of the generation mechanisms; the enhancement at the wave crests; the rapid settling of the largest drops; and the initial velocity of film, jet, and spume drops. Consequently, it is usually necessary to define a source height (effective height and effective flux), which is the height above the mean water level attained by the drops produced at the surface (interfacial flux). The effective flux, depending on the height considered, can be significantly lower than the interfacial flux, especially for the larger drops whose residence time is short and that do not attain heights more than a few meters, or may even remain within a wave height. For drops less than 1 μm, interfacial and effective fluxes are the same. Indeed, film and jet drops are ejected violently from the surface and quickly reach heights of several centimeters, where they can be transported and dispersed in the turbulent airflow. Spume droplets are ejected from the crest of breaking waves with initial velocities that are unknown but likely depend on the dynamics of the breaking wave front (Andreas et al. 2010, Mueller & Veron 2009b, Veron et al. 2012). For simplicity, the spray is assumed to be injected as a point source at height $h_0$, which can be taken as the height of breaking waves, for example (see **Figure 5**). In this case, one obtains $\bar{Q}_n = \bar{S}_0(r)\delta(z - h_0)$, where $\delta$ is the Dirac delta function. Hence, $\bar{S}_{n3} = \bar{S}_0(r)H(h_0 - z)$, with $H$ the Heaviside function, indicates that the spray generation function is uniform below the source height. Equation 39 then reads

$$\begin{aligned} \frac{\kappa u_* z f_s}{Sc_{tn}}\frac{\partial \bar{n}}{\partial z} + V_d \bar{n} &= 0 \quad \text{for} \quad z > h_0, \\ \frac{\kappa u_* z f_s}{Sc_{tn}}\frac{\partial \bar{n}}{\partial z} + V_d \bar{n} &= \bar{S}_0 \quad \text{for} \quad z < h_0. \end{aligned} \tag{40}$$

For $z > h_0$, Equation 40 simply states that the vertical transport of droplets by turbulence is balanced by gravitational settling. It can be solved and gives

$$\bar{n}(z) = \bar{n}(h_0)\left(\frac{z}{h_0}\right)^{\frac{-V_d Sc_{tn}}{\kappa u_* f_s}}. \tag{41}$$

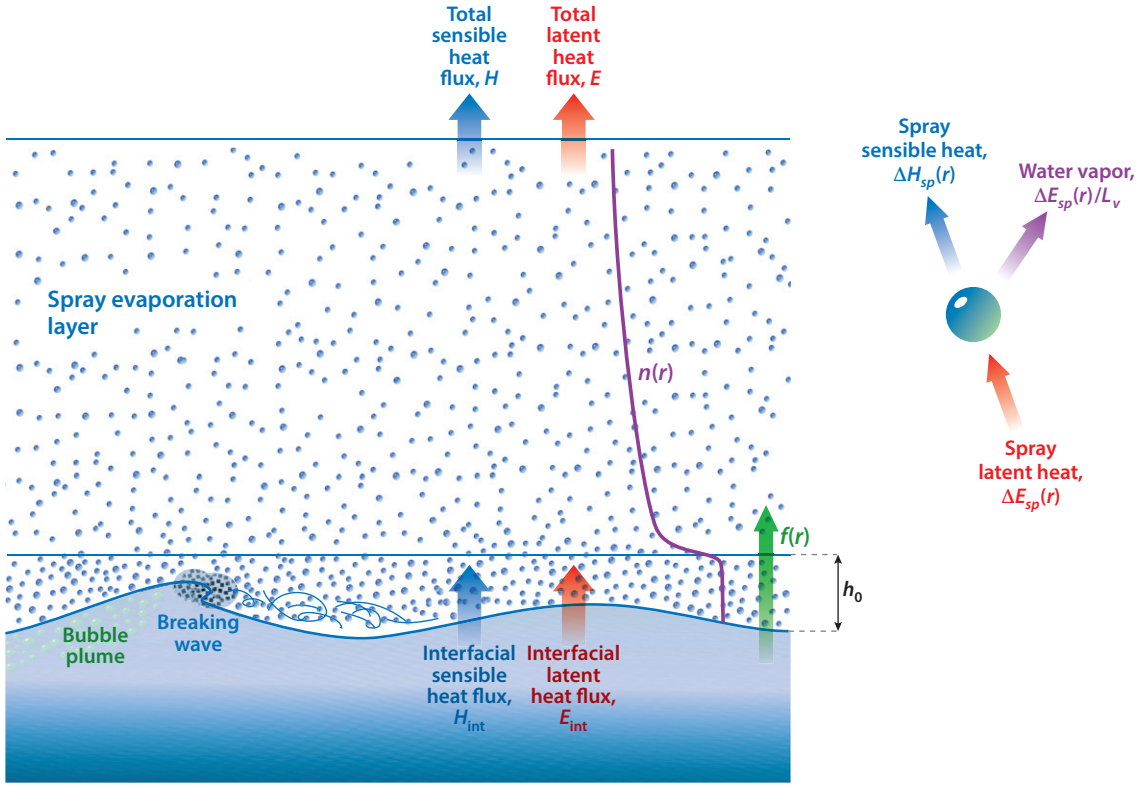


**Figure 5**

Schematic illustration of the spray evaporation layer, showing the interfacial, total, and spray-mediated heat fluxes.

For $z < h_0$, because the spray generation function is uniform under the source, the vertical gradient of $\bar{n}$ can be neglected (Fairall et al. 2009):

$$\bar{S}_0 = V_d \bar{n}(z). \tag{42}$$

Matching at $z = h_0$ leads to

$$\bar{S}_0 = V_d \bar{n}(h_0) = V_d \bar{n}(z) \left( \frac{z}{h_0} \right)^{\frac{V_d Sc_{tn}}{\kappa u_* f_s}}, \tag{43}$$

which offers a way to estimate the spray generation function $S_0$ from direct measurements of the mean droplet concentration $\bar{n}(z)$ (Fairall & Larsen 1984; de Leeuw 1986a,b, 1990, 1993; Lewis & Schwartz 2004).

## 4.4. Indirect Estimates of the Sea Spray Generation Function

The SSGF $dF(r)/dr$ is usually expressed as a function of the drop radius, and $f(r) = dF(r)/dr$ is typically parameterized as a function of local controlling parameters $dF(r)/dr = f(r, \alpha, \beta, \ldots)$. An obvious choice of parameter is the wind speed because breaking is intimately related to the wind speed (and fetch) and also the turbulence in the wind field will transport and suspend particles, thereby essentially controlling the effective flux. Although wind speed is a valuable and readily

measured proxy, several spray generation functions have also been developed using more fundamental parameters, such as whitecap coverage, wave age, surface stress, and fetch. A common assumption is that the shape of the source function is universal, whereas the number density in specific size ranges depends only on the controlling parameters. Thus, we obtain $f(r, \alpha, \beta, \ldots) = g(r)\phi(\alpha, \beta, \ldots)$.

Several spray generation functions have been derived using this approach. Monahan et al. (1982) first proposed a spray generation function based on laboratory drop measurements and the whitecap coverage data of Monahan & O'Muircheartaigh (1980). Later, Monahan et al. (1986) included laboratory data (Wu 1973, Lai & Shemdin 1974) to generate a spray generation function that included both bubble-generated drops and spume. The SSGF of Monahan et al. (1986) produces far too many spume droplets, however, and Andreas (1992) used a similar approach but with the field data of Wu et al. (1984) and Miller (1987). In turn, Fairall et al. (1994) proposed a spume generation function that also relied on a universal function of the drop radii $g(r)$. It seems unlikely that the shape, at the largest drop sizes, would be universal, especially considering that fragmentation dependence on the wind speed and turbulent intensity might play a role. Still, the recent data of Veron et al. (2012) do not show an expected transition in the SSGF at radii large enough to be broken up by the turbulence.

For droplets with $r_{80} \lesssim$ 10–20 μm, a great deal of progress in determining the SSGF has been made in the past decade. This is partly the result of improved measurement techniques that have narrowed down the uncertainties in previous SSGFs (Norris et al. 2012, 2013), as well as improved estimates of the whitecap coverage over a large range of wind speeds (Holthuijsen et al. 2012). The current state of knowledge has been well summarized by Lewis & Schwartz (2004), and de Leeuw et al. (2011) presented several additional SSGFs, showing that the estimates have indeed converged to within an order of magnitude or less in that drop radii range. **Figure 6** shows a subset of the available SSGFs in the literature for a 10-m equivalent wind speed of $U_{10} = 15$ m s$^{-1}$.

In comparison, very little is known about the SSGF for drops with $r_0 > 20$ μm. Andreas (2002) reviewed a dozen SSGFs and, based largely on energy arguments originally presented by Andreas et al. (1995), narrowed down the list to three SSGFs that had the proper wind-speed dependence. The SSGFs of Andreas (1992), Fairall et al. (1994), and Andreas (1998) were deemed appropriate. Andreas's (2002) work is encouraging because these SSGFs not only had the desired wind-speed dependence, they also had remarkably good agreement. **Figure 6** plots these three SSGFs along with recent estimates from Mueller & Veron (2009b) and Fairall et al. (2009). I note that Mueller & Veron's (2009b) estimate is calculated for $z = 10$ m and could differ substantially from the surface value. Although encouraging, the scatter in the available SSGF estimates for large droplets is still unsatisfactory. This is in large part a result of our lack of understanding of the actual generation mechanism by which spume drops are created and ejected into the airflow, thereby preventing the development of adequate physically based parameterizations.

The available data are also sparse at best (Anguelova et al. 1999, Veron et al. 2012). Yet, in an effort to develop physically based parameterizations of the spume generation function, recent work has departed from the use of the wind speed as a proxy and has explored the use of perhaps more fundamental parameters. For example, Zhao et al. (2006) proposed a wind-sea Reynolds number approach but still used the same universal $g(r)$ as in Andreas (1992, 1998) and Fairall et al. (1994). Another strategy has been to use $\Lambda(c)dc$, the length of a surface wave breaking front traveling at a speed in the range $[c, c + dc]$ originally introduced by Phillips (1985). Kudryavtsev (2006), Kudryavtsev & Makin (2009), and Mueller & Veron (2009b) used $\Lambda(c)dc$ to parameterize the spume generation function directly, with $\Lambda(c)dc$ dependent on the wind speed and fetch. Recently,

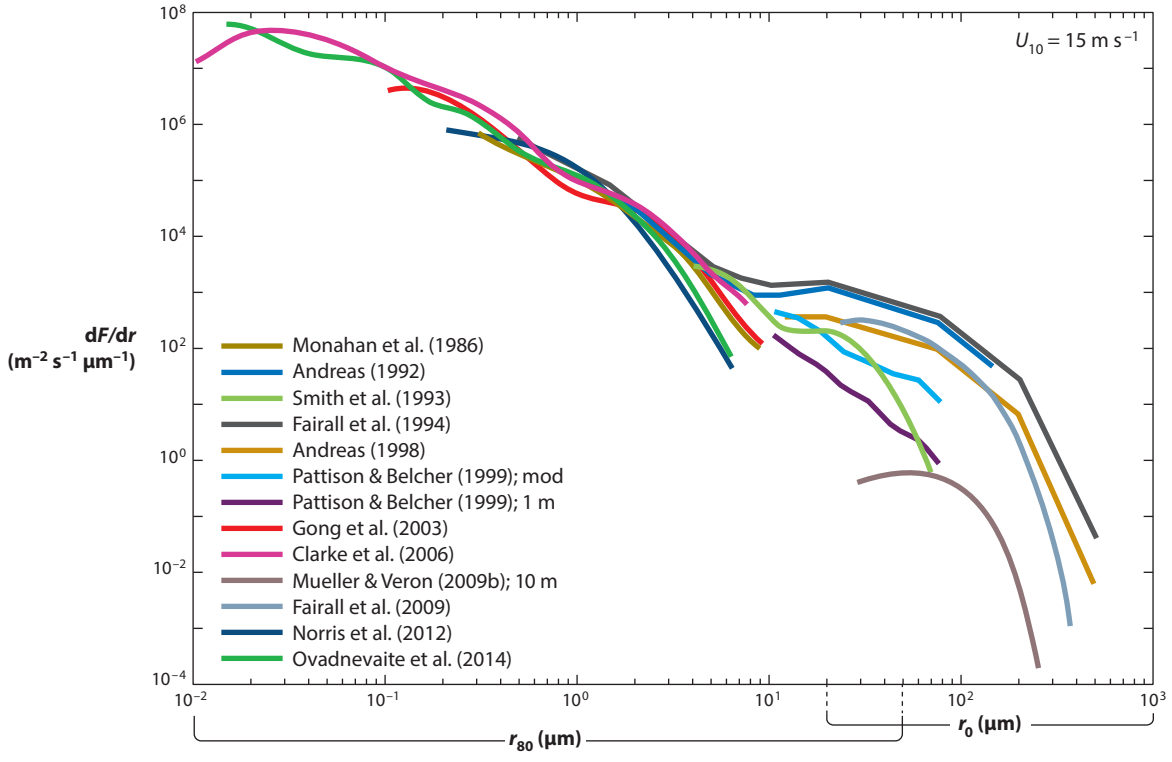


**Figure 6**

Size-dependent sea spray generation functions (number of droplets generated at the ocean's surface per unit surface per unit time and per unit radius) for a wind speed of $U_{10} = 15$ m s$^{-1}$ reported by various investigators.

Ovadnevaite et al. (2014) proposed an SSGF including a wave state–dependent Reynolds number based on field measurements.

## 5. SPRAY-INDUCED FLUXES

This section focuses on large spume droplets and briefly mentions their implications for the air-sea fluxes of momentum, heat, and water vapor. When large spume drops are generated at the surface and subsequently transported in the ABL, they exchange momentum with the airflow. The spray-mediated momentum flux can be estimated using Equation 11 and the SSGF:

$$\boldsymbol{\tau}_{\mathrm{sp}} = \int \Delta \mathbf{p}_{\mathrm{sp}}(r) \frac{dF(r)}{dr} dr. \tag{44}$$

Andreas (2004) estimated that the spray carries approximately 10% of the total air-sea stress at $U_{10} = 25$–$30$ m s$^{-1}$ and rivals the momentum flux from the wind at approximately $U_{10} = 60$ m s$^{-1}$. Innocentini & Gonçalves (2010) in turn found that the spray carries approximately 20% of the total air-sea stress at $U_{10} = 60$ m s$^{-1}$, whereas Mueller & Veron (2014b) found that the spume has a 10% effect on the momentum flux, regardless of the wind speed.

In addition, Richter & Sullivan (2013) found that when the droplet concentration is sufficiently high, spray can carry a substantial amount of the total air-sea stress. However, they also found

**Tropical cyclone:** a rapidly rotating storm system characterized by strong winds and a low pressure center; also referred to as a hurricane or typhoon

that the spray essentially redistributes the stress within the boundary layer, as was previously postulated by Andreas (2004). Indeed, as the droplets accelerate or decelerate during their flight within the ABL, the airflow must in turn decelerate or accelerate. The spray thus modifies the near-surface wind speed profile and can therefore alter the air-sea drag. Accordingly, the total air-sea momentum flux is estimated from the interfacial stress, $\boldsymbol{\tau}_{\text{int}}$, and the spray-mediated stress $\boldsymbol{\tau}_{\text{sp}}$ using

$$\boldsymbol{\tau} = \boldsymbol{\tau}_{\text{int}} + \boldsymbol{\tau}_{\text{sp}}(1 + \gamma_1), \tag{45}$$

where $\gamma_1$ accounts for the spray-induced modifications to the interfacial flux because of the modification of the wind speed profile.

In the context of tropical cyclones, as mentioned in Section 3.2, spray effects have been offered as a potential candidate to explain the reduction of the air-sea drag coefficient at high wind speeds (Powell et al. 2003, Donelan et al. 2004, Bell et al. 2012). However, the scatter in the estimated drag coefficients among the studies at wind speeds higher than $U_{10} = 30\ \text{m s}^{-1}$ (Andreas 2004, Kudryavtsev & Makin 2011, Bao et al. 2011, Rastigejev et al. 2011, Mueller & Veron 2014b) suggests that these estimates are quite sensitive to the spray concentration and the large uncertainties associated with the SSGF at these wind speeds.

As for the heat flux, although sea spray was thought to play a role in the air-sea fluxes of latent and sensible heat since the 1970s, Andreas (1992) was the first to offer a robust quantitative estimate of the spray-mediated heat fluxes. Andreas (1992) offered estimates based on an SSGF deduced from field data and estimates of drop exchanges (Equation 18) and concluded that the spray latent heat flux is substantial. Several subsequent studies followed (Fairall et al. 1994, Edson et al. 1996, Andreas & DeCosmo 1999, Andreas 2002, Andreas et al. 2008, Mueller & Veron 2014b). In most of these studies, the authors considered the spray-mediated sensible and latent heat fluxes, $H_{\text{sp}}$ and $E_{\text{sp}}$, respectively. These are obtained from Equation 18 and by using an SSGF:

$$\begin{aligned} H_{\text{sp}} &= \int \Delta H_{\text{sp}}(r) \frac{dF(r)}{dr} dr, \\ E_{\text{sp}} &= \int \Delta E_{\text{sp}}(r) \frac{dF(r)}{dr} dr. \end{aligned} \tag{46}$$

Following Fairall et al. (1994), most studies have attempted to include the spray feedback effects, that is, the influence of the spray on the boundary layer. Succinctly, when a spray droplet is ejected in the near-surface boundary layer (referred to as the spray evaporation layer; see **Figure 5**), it rapidly exchanges sensible heat with the atmosphere, $\Delta H_{\text{sp}}(r)$, and cools to a temperature below the atmospheric temperature, thus warming the air. Subsequently, the spray droplet will start evaporating, thereby extracting latent heat from the atmosphere, $\Delta E_{\text{sp}}(r)$. In turn, the energy required to evaporate the drop must necessarily come from the atmosphere in the spray evaporation layer (Fairall et al. 1994). Hence, the evaporation of the drop also cools the air by $\Delta E_{\text{sp}}(r)$. In short, the spray-mediated net sensible heat flux is $H_{\text{sp}} - E_{\text{sp}}$.

I note here that both $\Delta H_{\text{sp}}(r)$ and $\Delta E_{\text{sp}}(r)$ are cubic functions of $r$. This means that the spray heat fluxes are in fact proportional to the sea spray volume generation function, $\frac{4\pi}{3} r^3 dF(r)/dr$, that is, the volume of water ejected per unit surface of ocean surface per unit time (per radius increment). Unfortunately, this means that uncertainties in $dF(r)/dr$ at large radii will be exacerbated for $r^3 dF(r)/dr$, thereby rendering estimates of $H_{\text{sp}}$ and $E_{\text{sp}}$ difficult and perhaps still doubtful at this point.

In turn, these spray fluxes alter the temperature profiles and humidity content of the spray evaporation layer and will therefore influence the traditional boundary layer fluxes at the interface, $H_{\text{int}}$ and $E_{\text{int}}$. One typically accounts for these feedback effects by introducing feedback coefficients.

The sensible and latent heat fluxes at the top of the evaporation layer are then given as

$$\begin{aligned} H &= H_{\text{int}} + H_{\text{sp}}(1+\eta_1) - E_{\text{sp}}(1+\eta_2), \\ E &= E_{\text{int}} + E_{\text{sp}}(1+\varepsilon_1), \end{aligned} \tag{47}$$

where $\varepsilon_1$, $\eta_1$, and $\eta_2$ account for the spray-induced modifications to the interfacial heat fluxes. If the spray fluxes and the feedback can be parameterized, the total fluxes can be used as bottom boundary conditions for operational weather models and would account for the spray without necessarily dealing with the details of transfer processes within the evaporation layer.

Most studies of spume-mediated heat flux have focused on doing exactly that to understand and predict intense and local weather events such as tropical cyclones. For example, Bao et al. (2000) showed an increased storm intensity when including spray evaporation, an effect that is somewhat tempered when the spray takes the heat for evaporation from the near-surface layers. Andreas & Emanuel (2001) demonstrated that the sensible heat flux is a critical parameter for sustaining hurricanes, and Liu et al. (2010) also found the intensification of tropical cyclones with a fully coupled atmosphere-ocean model. Overall, Andreas et al. (2008, 2010) concluded that the spray latent and sensible heat fluxes overcome the interfacial fluxes at wind speeds of approximately $U_{10} = 25$–$30$ m s$^{-1}$. There seems to be a consensus that high wind speeds generate a substantial amount of large spume droplets, thereby increasing the air-sea enthalpy fluxes and thus having a positive feedback on storm intensification. At these wind speeds, however, shifts in the drop size affect the turbulent kinetic energy and thermodynamic balances. For example, Bianco et al. (2011) showed that whereas small drops evaporate at moderate wind speeds, large drops present in high winds enhance the sensible heat flux (Andreas & Emanuel 2001). Rosenfeld et al. (2012) also suggested that small sea spray droplets might play an indirect role in tropical cyclone intensity through the generation of cloud condensation nuclei and rain. As of now, with the uncertainty still associated with the SSGF of large droplets, particularly in high winds (see **Figure 6**), a definitive quantitative assessment of spray effects on tropical cyclone intensity remains out of reach.

## 6. SUMMARY

In recent years, it has become recognized that surface wave and wave breaking–related phenomena are crucial participants in the coupling of the atmosphere and ocean (Melville 1996, Sullivan & McWilliams 2010). At wind speeds at which breaking becomes frequent, sea spray is generated at the surface and ejected into the airflow in which it transfers sensible and latent heat and gets transported into the ABL. During this transport, spray drops will also participate in the chemical cycle and radiative atmospheric balances (Mulcahy et al. 2008, Vaishya et al. 2012). The spray is generated through two pathways: bubble breakup and direct surface detachment, both of which are induced by wave breaking. Simplistically, small and medium-size droplets in the atmosphere are likely to be film and jet drops originating from the bubble breakup generation mechanism. These drops have residence times of hours to days and will get transported away from the interface and higher in the atmosphere, where they will participate in the global aerosol cycle. These drops' contributions to the air-sea heat and momentum fluxes are likely to be modest; however, the droplets themselves are the principal source of atmospheric sea salt aerosols. The largest drops found in the ABL are spume drops ejected from the crest of breaking waves. Their residence time is on the order of seconds to minutes, and they get transported over relatively short distances within the ABL. As such, their influence is local. Because of their large surface area, volume, and mass, these drops are likely to participate significantly in the air-sea fluxes of momentum, sensible heat, and latent heat.

The past decade has seen tremendous progress in evaluating the SSGF for small and medium-size drops, and a consensus has emerged (see **Figure 6**) (Lewis & Schwartz 2004, de Leeuw et al. 2011). The biochemical compositions and implications of these drops in the global aerosol cycle and radiation balance continue to be challenging, however. As for large drops, several obstacles remain. A large scatter persists in the spume generation function; thus, there is little agreement on the spray's overall effects on the air-sea momentum and enthalpy fluxes. This is especially true at higher wind speeds, for example, those greater than $U_{10} = 30$ m s$^{-1}$, for which we expect spray fluxes to have an important role in storm and hurricane meteorology. Unfortunately, these are also the speeds at which the combined effects of the spray (and the feedback) on the air-sea momentum and enthalpy fluxes are not yet well resolved.



## FUTURE ISSUES

1. There is a clear need to continue to study large spume drops and, in particular, their generation mechanism. Details on the generation mechanism, initial velocity, residence time, and dynamic behavior through the airflow are critical to the development of adequate parameterizations.
2. Future parameterizations of the spray generation functions should seek to use fundamental breaking parameters such as $\Lambda(c)dc$, the moments of which can describe the length of breaking fronts and their speed (spume drops), the area covered by whitecaps (film and jet drops), and the energy dissipated, which in turn can be related to the volume of air entrained (bubble clouds, film and jet drops).
3. Large eddy simulation models of the atmospheric and oceanic boundary layer have come to maturity, and they should be employed in future studies, perhaps allowing for hybrid Eulerian-Lagrangian approaches incorporating small-scale dynamics, vertical transport by large boundary layer structures, and feedback effects.
4. Small film and jet droplets transport significant amounts of organic matter and inorganic chemical species. It is likely that the size-dependent biochemical compositions need to be included in the source functions for the smallest droplets to better estimate their aggregated impact on the global aerosol cycle (Long et al. 2011).
5. To that effect, controlled laboratory experiments are needed to evaluate what other parameters, such as salinity, ionic composition, surface-active material, and temperature, influence the formation and composition of spray (Sellegri et al. 2006, Ault et al. 2013, Stokes et al. 2013).
6. Regional variability [e.g., in the coastal ocean (Piazzola et al. 2009, Saruwatari & Abe 2014)], as well as seasonal fluctuations in spray generation and subsequent dynamics and thermodynamics effects, needs to be better addressed.
7. The global climate effects of spray are starting to emerge, in particular because of its influence on the global radiative balance. However, studies on the repercussions and potential feedbacks on global warming are sporadic. From a societal point of view, sea spray implications on human health are occasionally reported, but systematic studies are still needed.

## DISCLOSURE STATEMENT

The author is not aware of any biases that might be perceived as affecting the objectivity of this review.

## ACKNOWLEDGMENTS

I wish to thank my academic mentor, Ken Melville, for his support and encouragement over the years and getting me involved in this field in the first place. I also wish to acknowledge James Mueller, who has kept me interested in sea spray over the years. I have had many helpful discussions over the past few years with Ed Andreas and Chris Fairall, both of whom have supported and encouraged my work on sea spray. Gerrit de Leeuw and Ernie Lewis have generously provided data for **Figure 6**. I wish to thank Dana Veron who proofed several versions of the original manuscript, and Ed Andreas and David Richter, who offered comments. My work in the area of air-sea interaction has been supported over the years by grants from the National Science Foundation, the Office of Naval Research, the National Oceanic and Atmospheric Administration, and the Department of Energy. Finally, I wish to thank the Co-Editors of the *Annual Review of Fluid Mechanics* for inviting me to submit this review.

## LITERATURE CITED

Afeti GM, Resch FJ. 1990. Distribution of the liquid aerosol produced from bursting bubbles in sea and distilled water. *Tellus B* 42:378–84

Aller JY, Kuznetsova MR, Jahns CJ, Kemp PF. 2005. The sea surface microlayer as a source of viral and bacterial enrichment in marine aerosols. *J. Aerosol Sci.* 36:801–12

Andreae ML, Rosenfeld D. 2008. Aerosol-cloud-precipitation interactions. Part 1. The nature and sources of cloud-active aerosols. *Earth Sci. Rev.* 89:13–44

**Andreas EL. 1989. *Thermal and size evolution of sea spray droplets*. CRREL Rep. 89-11, US Army Corps Eng., Cold Reg. Res. Eng. Lab., Hanover, NH**

Andreas EL. 1990. Time constants for the evolution of sea spray droplets. *Tellus B* 42:481–97

Andreas EL. 1992. Sea spray and the turbulent air-sea heat fluxes. *J. Geophys. Res.* 97:11429–41

Andreas EL. 1995. The temperature of evaporating sea spray droplets. *J. Atmos. Sci.* 52:852–62

Andreas EL. 1998. A new sea spray generation function for wind speeds up to 32 m $s^{-1}$. *J. Phys. Oceanogr.* 28:2175–84

Andreas EL. 2002. A review of the sea spray generation function for the open ocean. In *Atmosphere-Ocean Interactions*, Vol. 1, ed. WA Perrie, pp. 1–46. Southhampton, UK: WIT

Andreas EL. 2004. Spray stress revisited. *J. Phys. Oceanogr.* 34:1429–40

Andreas EL. 2005. Approximation formula for the microphysical properties of saline droplets. *Atmos. Res.* 75:323–45

Andreas EL. 2011. Fallacies of the enthalpy transfer coefficient over the ocean in high winds. *J. Atmos. Sci.* 68:1435–45

Andreas EL, DeCosmo J. 1999. Sea spray production and influence on air-sea heat and moisture fluxes over the open ocean. In *Air-Sea Exchange: Physics, Chemistry and Dynamics*, ed. GL Geernaert, pp. 327–62. Dordrecht: Kluwer Acad.

Andreas EL, Edson JB, Monahan EC, Rouault MP, Smith SD. 1995. The spray contribution to net evaporation from the sea: a review of recent progress. *Bound.-Layer Meteorol.* 72:3–52

Andreas EL, Emanuel KA. 2001. Effects of sea spray on tropical cyclone intensity. *J. Atmos. Sci.* 58:3741–51

Andreas EL, Jones KF, Fairall CW. 2010. Production velocity of sea spray droplets. *J. Geophys. Res.* 115:C12065

Andreas EL, Persson POG, Hare JE. 2008. A bulk turbulent air-sea flux algorithm for high-wind, spray conditions. *J. Phys. Oceanogr.* 38:1581–96

Anguelova M, Barber RP, Wu J. 1999. Spume drops produced by the wind tearing of wave crests. *J. Phys. Oceanogr.* 29:1156–65

**Derives the temperature and radius evolution for saline droplets based on the work of Pruppacher & Klett (1978).**

Ault AP, Moffet RC, Baltrusaitis J, Collins DB, Ruppel MJ, et al. 2013. Size-dependent changes in sea spray aerosol composition and properties with different seawater conditions. *Environ. Sci. Technol.* 47:5603–12

Auton TR, Hunt JCR, Prud'Homme M. 1988. The force exerted on a body in inviscid unsteady non-uniform rotational flow. *J. Fluid Mech.* 197:241–57

Bao JW, Fairall CW, Michelson SA, Bianco L. 2011. Parameterizations of sea-spray impact on the air-sea momentum and heat fluxes. *Mon. Weather Rev.* 139:3781–97

Bao JW, Wilczak JM, Choi JK, Kantha LH. 2000. Numerical simulations of air-sea interaction under high wind conditions using a coupled model: a study of hurricane development. *Mon. Weather Rev.* 128:2190–210

Barenblatt GI, Chorin AJ, Prostokishin VM. 2005. A note concerning the Lighthill "sandwich model" of tropical cyclones. *Proc. Natl. Acad. Sci. USA* 102:11148–50

Bell MM, Montgomery MT, Emanuel KA. 2012. Air-sea enthalpy and momentum exchange at major hurricane wind speeds observed during CBLAST. *J. Atmos. Sci.* 69:3197–222

Bianco L, Bao JW, Fairall CW, Michelson SA. 2011. Impact of sea-spray on the atmospheric surface layer. *Bound.-Layer Meteorol.* 140:361–81

Bigg EK, Leck C. 2008. The composition of fragments of bubbles bursting at the ocean surface. *J. Geophys. Res.* 113:D11209

Bird JC, de Ruitier R, Courbin L, Stone HA. 2010. Daughter bubble cascades produced by folding of ruptured thin films. *Nature* 465:759–62

Extracted from Blanchard's PhD thesis work, this paper relaunched modern scientific interest in sea spray.

**Blanchard DC. 1963. The electrification of the atmosphere by particles from bubbles in the sea. *Prog. Oceanogr.* 1:71–202**

Blanchard DC. 1964. Sea-to-air transport of surface active material. *Science* 146:396–97

Blanchard DC. 1989. The size and height to which jet drops are ejected from bursting bubbles in sea water. *J. Geophys. Res.* 94:10999–1002

Blanchard DC, Syzdek LD. 1972. Concentration of bacteria in jet drops from bursting bubbles. *J. Geophys. Res.* 77:5087–99

Blanchard DC, Syzdek LD. 1988. Film drop production as a function of bubble size. *J. Geophys. Res.* 93:3649–54

Bondur VG, Sharkov EA. 1982. Statistical properties of whitecaps on a rough sea. *Oceanology* 22:274–79

Bye JAT, Jenkins AD. 2006. Drag coefficient reduction at very high wind speeds. *J. Geophys. Res.* 111: C03024

Presents comprehensive experiments on spray generated by laboratory breaking waves.

**Cipriano RJ, Blanchard DC. 1981. Bubble and aerosol spectra produced by a laboratory breaking wave. *J. Geophys. Res.* 86:8085–92**

Clarke AD, Owens SR, Zhou J. 2006. An ultrafine sea-salt flux from breaking waves: implications for cloud condensation nuclei in the remote marine atmosphere. *J. Geophys. Res.* 111:D06202

Clift R, Gauvin WH. 1970. The motion of particles in turbulent gas streams. *Proc. Chemeca 1970*, pp. 14–28. London: Butterworth

Crowe C, Sommerfeld M, Tsuji Y. 1998. *Multiphase Flows with Droplets and Particles*. Boca Raton, FL: CRC

Cunningham E. 1910. On the velocity of steady fall of spherical particles through fluid medium. *Proc. R. Soc. Lond. A* 83:357–65

Davies CN. 1945. Definitive equations for the fluid resistance of spheres. *Proc. Phys. Soc. Lond.* 57:259–70

de Leeuw G. 1986a. Size distributions of giant aerosol particles close above sea level. *J. Aerosol Sci.* 17:293–96

de Leeuw G. 1986b. Vertical profiles of giant particles close above the sea surface. *Tellus B* 38:51–61

de Leeuw G. 1990. Profiling of aerosol concentrations, particle size distribution and relative humidity in the atmospheric surface layer over the North Sea. *Tellus B* 42:342–54

de Leeuw G. 1993. Aerosols near the air-sea interface. *Trends Geophys. Res.* 2:55–70

Presents a recent review on fluxes associated with film and jet drops.

**de Leeuw G, Andreas EL, Anguelova MD, Fairall CW, Lewis ER, et al. 2011. Production flux of sea spray aerosol. *Rev. Geophys.* 49:RG2001**

Deane G, Stokes MD. 2002. Scale dependence of bubble creation mechanisms in breaking waves. *Nature* 418:839–44

Donelan MA, Haus BK, Reul N, Plant WJ, Stiassnie M, et al. 2004. On the limiting aerodynamic roughness of the ocean in very strong winds. *Geophys. Res. Lett.* 31:L18306

Edson JB, Anquetin S, Mestayer PG, Sini JF. 1996. Spray droplet modeling. 2. An interactive Eulerian-Lagrangian model of evaporating spray droplets. *J. Geophys. Res.* 101:1279–93

Edson JB, Fairall CW. 1994. Spray droplet modeling. 1. Lagrangian model simulation of the turbulent transport of evaporating droplets. *J. Geophys. Res.* 99:25295–311
Facchini MC, Rinaldi M, Decesari S, Carbone C, Finessi E, et al. 2008. Primary submicron marine aerosol dominated by insoluble organic colloids and aggregates. *J. Geophys. Res.* 35:L17814
Fairall CW, Banner ML, Peirson WL, Asher W, Morison RP. 2009. Investigation of the physical scaling of sea spray spume droplet production. *J. Geophys. Res.* 114:C10001
**Fairall CW, Kepert JD, Holland GJ. 1994. The effect of sea spray on surface energy transports over the ocean. *Global Atmos. Ocean Syst.* 2:121–42**
Fairall CW, Larsen SE. 1984. Dry deposition, surface production, and dynamics of aerosols in the marine boundary layer. *Atmos. Environ.* 18:69–77
Fitzgerald JW. 1975. Approximation formulas for the equilibrium size of an aerosol particle as a function of its dry size and composition and the ambient relative humidity. *J. Appl. Meteorol.* 14:1044–49
Fleming LE, Backer LC, Baden DG. 2005. Overview of aerosolized Florida red tide toxins: exposures and effects. *Environ. Health Perspect.* 113:618–20
Fuentes E, Coe H, Green D, de Leeuw G, McFiggans G. 2010. Laboratory-generated primary marine aerosol via bubble-bursting and atomization. *Atmos. Meas. Tech.* 3:141–62
Gong SL, Barrie LA, Blanchet JP. 1997. Modeling sea-salt aerosols in the atmosphere. 1. Model development. *J. Geophys. Res.* 102:3805–18
Gong SL, Barrie LA, Blanchet JP. 2003. A parameterization of sea-salt aerosol source function for sub- and super-micron particles. *Global Biogeochem. Cycles* 17:1097
Goroch A, Burk S, Davidson KL. 1980. Stability effects on aerosol size and height distributions. *Tellus* 32:245–50
Holthuijsen LH, Powell MD, Pietrzak JD. 2012. Wind and waves in extreme hurricanes. *J. Geophys. Res.* 117:C09003
Hoppel WA, Frick GM, Fitzgerald JW. 2002. Surface source function for sea-salt aerosol and aerosol dry deposition to the ocean surface. *J. Geophys. Res.* 107(D19):4382
Innocentini V, Gonçalves IA. 2010. The impact of spume droplets and wave stress parameterizations on simulated near-surface maritime wind and temperature. *J. Phys. Oceanogr.* 40:1373–89
Keene WC, Maring H, Maben JR, Kieber DJ, Pszenny AAP, et al. 2007. Chemical and physical characteristics of nascent aerosols produced by bursting bubbles at a model air-sea interface. *J. Geophys. Res.* 112:D21202
Kepert JD, Fairall CW, Bao JW. 1999. Modeling the interaction between the atmospheric boundary layer and evaporating sea spray droplets. In *Air-Sea Exchange: Physics, Chemistry and Dynamics*, ed. GL Geernaert, pp. 363–409. Dordrecht: Kluwer Acad.
Kientsler CF, Arons AB, Blanchard DC, Woodcock AH. 1954. Photographic investigation of the projection of droplets by bubbles bursting at a water surface. *Tellus* 6:1–7
Kiger KT, Duncan JH. 2012. Air-entrainment mechanisms in plunging jets and breaking waves. *Annu. Rev. Fluid Mech.* 44:563–96
Kleiss JM, Melville WK. 2011. The analysis of sea surface imagery for whitecap kinematics. *J. Atmos. Oceanic Technol.* 28:219–43
Koga M. 1981. Direct production of droplets from breaking wind-waves: its observation by a multi-colored overlapping exposure photographing technique. *Tellus* 33:552–63
Kudryavtsev VN. 2006. On the effect of sea drops on the atmospheric boundary layer. *J. Geophys. Res.* 111:C07020
Kudryavtsev VN, Makin VK. 2009. Model of the spume sea spray generation. *Geophys. Res. Lett.* 36:289–303
Kudryavtsev VN, Makin VK. 2011. Impact of ocean spray on the dynamics of the marine atmospheric boundary layer. *Bound.-Layer Meteorol.* 140:383–410
Lai RJ, Shemdin OH. 1974. Laboratory study of the generation of spray over water. *J. Geophys. Res.* 79:3055–63
**Lewis ER, Schwartz SE. 2004. *Sea Salt Aerosol Production: Mechanisms, Methods, Measurements, and Models*. Washington, DC: Am. Geophys. Union**
Lhuissier H, Villermaux E. 2012. Bursting bubble aerosols. *J. Fluid Mech.* 696:5–44
Liu B, Guan C, Xie L. 2012. The wave state and sea spray related parameterization of wind stress applicable from low to extreme winds. *J. Geophys. Res. Oceans* 117:C00J22

**Presents what is considered to date to be the most reliable source function for spume.**

**Provides an extensive review of sea salt aerosols.**

Liu B, Liu H, Xie L, Guan C, Zhao D. 2010. A coupled atmosphere–wave–ocean modeling system: simulation of the intensity of an idealized tropical cyclone. *Mon. Weather Rev.* 139:132–52

Long MS, Keene WC, Kieber DJ, Erickson DJ, Maring H. 2011. A sea-state based source function for size- and composition-resolved marine aerosol production. *Atmos. Chem. Phys.* 11:1203–16

MacIntyre F. 1972. Flow patterns in breaking bubbles. *J. Geophys. Res.* 77:5211–28

Magnaudet J, Rivero M, Fabre J. 1995. Accelerated flow past a rigid sphere or a spherical bubble. Part 1. Steady straining flow. *J. Fluid Mech.* 284:97–135

Makin VK. 2005. A note on the drag of the sea surface at hurricane winds. *Bound.-Layer Meteorol.* 115:169–76

Marmottant PH, Villermaux E. 2004. On spray formation. *J. Fluid Mech.* 498:73–111

Mårtensson M, Nilson ED, de Leeuw G, Cohen LH, Hansson HC. 2003. Laboratory simulations and parameterization of the primary marine aerosol production. *J. Geophys. Res.* 108:4297

**Presents a thorough derivation of the equation of motion for a single drop.**

**Maxey MR, Riley JJ. 1983. Equation of motion for a small rigid sphere in a nonuniform flow. *Phys. Fluids* 26:883–89**

Meek CC, Jones BG. 1973. Studies of the behavior of heavy particles in a turbulent fluid flow. *J. Atmos. Sci.* 30:239–44

Meirink J. 2002. *The role of wind waves and sea spray on air-sea interaction*. PhD Diss., Tech. Univ. Delft

Melville WK. 1996. The role of surface-wave breaking in air-sea interaction. *Annu. Rev. Fluid Mech.* 28:279–321

Mestayer PG, Van Eijk AMJ, de Leeuw G, Tranchant BS. 1996. Numerical simulation of the dynamics of sea spray over the waves. *J. Geophys. Res.* 101:20771–97

Miller MA. 1987. *An investigation of aerosol generation in the marine planetary boundary layer*. MS Thesis, Pa. State Univ.

Modini RL, Russell LM, Deane GB, Stokes MD. 2013. Effect of soluble surfactant on bubble persistence and bubble-produced aerosol particles. *J. Geophys. Res.* 118:1388–400

Monahan EC. 1971. Oceanic whitecaps. *J. Phys. Oceanogr.* 1:139–44

Monahan EC, Davidson KL, Spiel DE. 1982. Whitecap aerosol productivity deduced from simulation tank measurements. *J. Geophys. Res.* 87:8898–904

**A seminal paper on whitecap coverage.**

**Monahan EC, O'Muircheartaigh I. 1980. Optimal power-law description of oceanic whitecap coverage dependence on wind speed. *J. Phys. Oceanogr.* 10:2094–99**

Monahan EC, O'Muircheartaigh I. 1986. Whitecaps and the passive remote sensing of the ocean surface. *Int. J. Remote Sens.* 7:627–42

Monahan EC, Spiel D, Davidson K. 1986. A model of marine aerosol generation via whitecaps and wave disruption. In *Oceanic Whitecaps*, ed. EC Monahan, G Niocaill, pp. 167–74. New York: Springer

Mueller JA, Veron F. 2009a. A Lagrangian stochastic model for heavy particle dispersion in the atmospheric marine boundary layer. *Bound.-Layer Meteorol.* 130:229–47

Mueller JA, Veron F. 2009b. A sea state–dependent spume generation function. *J. Phys. Oceanogr.* 39:2363–72

Mueller JA, Veron F. 2010. A Lagrangian stochastic model for sea-spray evaporation in the atmospheric marine boundary layer. *Bound.-Layer Meteorol.* 137:135–52

Mueller JA, Veron F. 2014a. Impact of sea spray on air-sea fluxes part 1: results from stochastic simulations of sea spray drops over the ocean. *J. Phys. Oceanogr.* In press

Mueller JA, Veron F. 2014b. Impact of sea spray on air-sea fluxes part 2: feedback effects. *J. Phys. Oceanogr.* In press

Mulcahy JP, O'Dowd CD, Jennings SG, Ceburnis D. 2008. Significant enhancement of aerosol optical depth in marine air under high wind conditions. *Geophys. Res. Lett.* 35:L16810

Norris SJ, Brooks IM, Hill MK, Brooks BJ, Smith MH, Sproson DAJ. 2012. Eddy covariance measurements of the sea spray aerosol flux over the open ocean. *J. Geophys. Res.* 117:D07210

Norris SJ, Brooks IM, Yelland MJ, de Leeuw G, Pascal RW, Brooks B. 2013. Near-surface measurements of sea spray aerosol production over whitecaps in the open ocean. *Ocean Sci.* 9:144–45

O'Dowd CD, de Leeuw G. 2007. Marine aerosol production: a review of the current knowledge. *Philos. Trans. R. Soc. A* 367:1753–74

Ovadnevaite J, Manders A, de Leeuw G, Ceburnis D, Monahan C, et al. 2014. A sea spray aerosol flux parameterization encapsulating wave state. *Atmos. Chem. Phys.* 14:1837–52

Pattison MJ, Belcher SE. 1999. Production rates of sea-spray droplets. *J. Geophys. Res.* 104:18397–407
Phillips OM. 1985. Spectral and statistical properties of the equilibrium range in wind-generated gravity waves. *J. Fluid Mech.* 156:505–31
Piazzola J, Forget P, Lafon C, Despiau S. 2009. Spatial variation of sea-spray fluxes over a Mediterranean coastal zone using a sea-state model. *Bound.-Layer Meteorol.* 132:167–83
Pilch M, Erdman CA. 1987. Use of breakup time and velocity history data to predict the maximum size of stable fragments for acceleration-induced breakup of a liquid drop. *Int. J. Multiphase Flow* 13:741–57
Powell MD, Vickery PJ, Reinhold TA. 2003. Reduced drag coefficient for high wind speeds in tropical cyclones. *Nature* 422:279–83
Prosperetti A, Oguz HN. 1993. The impact of drops on liquid surfaces and the underwater noise of rain. *Annu. Rev. Fluid Mech.* 25:577–602
Pruppacher HR, Klett JD. 1978. *Microphysics of Clouds and Precipitation*. Dordrecht: D. Riedel
Pruppacher HR, Klett JD. 1997. *Microphysics of Clouds and Precipitation*. Dordrecht: Kluwer. 997 pp. 2nd ed.
Rastigejev Y, Suslov S, Lin YL. 2011. Effect of ocean spray on vertical momentum transport under high-wind conditions. *Bound.-Layer Meteorol.* 141:1–20
Resch FJ, Afeti GM. 1991. Film drop distributions from bubbles bursting in sea water. *J. Geophys. Res.* 96:10681–88
Resch FJ, Darrozes JS, Afeti GM. 1986. Marine liquid aerosol production from bursting of air bubbles. *J. Geophys. Res.* 91:1019–29
Richter DH, Sullivan PP. 2013. Sea surface drag and the role of spray. *Geophys. Res. Lett.* 40:656–60
Richter DH, Sullivan PP. 2014. The sea spray contribution to sensible heat flux. *J. Atmos. Sci.* 71:640–54
Rosenfeld D, Woodley WL, Khain A, Cotton WR, Carrio G, et al. 2012. Aerosol effects on microstructure and intensity of tropical cyclones. *Bull. Am. Meteorol. Soc.* 93:987–1001
Rouault MP, Mestayer PG, Schiestel R. 1991. A model of evaporating spray droplet dispersion. *J. Geophys. Res.* 96:7181–200
Saruwatari A, Abe N. 2014. Relationship between latent heat of sea spray and uncertainty of a meteorological field. *Appl. Ocean Res.* 44:102–11
Seinfeld JH, Pandis SN. 1998. *Atmospheric Chemistry and Physics: From Air Pollution to Climate*. New York: Wiley
Sellegri K, O'Dowd CD, Yoon YJ, Jennings SG, de Leeuw G. 2006. Surfactants and submicron sea spray generation. *J. Geophys. Res.* 111:D22215
Shaw RA. 2003. Particle-turbulence interactions in atmospheric clouds. *Annu. Rev. Fluid Mech.* 35:183–227
Shpund J, Pinsky M, Khain A. 2011. Microphysical structure of the marine boundary layer under strong wind and spray formation as seen from simulations using a 2D explicit microphysical model. Part I: The impact of large eddies. *J. Atmos. Sci.* 68:2366–84
Shpund J, Zhang JA, Pinsky M, Khain A. 2012. Microphysical structure of the marine boundary layer under strong wind and spray formation as seen from simulations using a 2D explicit microphysical model. Part II: The role of sea spray. *J. Atmos. Sci.* 69:3501–14
Slinn SA, Slinn WGN. 1980. Prediction for particle deposition on natural waters. *Atmos. Env.* 14:1013–16
Slinn WGN, Hasse L, Hicks B, Hogan A, Lal D, et al. 1978. Some aspects of the transfer of atmospheric trace constituents past the air-sea interface. *Atmos. Environ.* 12:2055–87
Smith MH, Park PM, Consterdine IE. 1993. Marine aerosol concentration and estimated fluxes over the sea. *Q. J. R. Meteorol. Soc.* 119:809–24
Spiel DE. 1994a. The number and size of jet drops produced by air bubbles bursting on a fresh water surface. *J. Geophys. Res.* 99:10289–96
Spiel DE. 1994b. The sizes of jet drops produced by air bubbles bursting on sea- and fresh-water surfaces. *Tellus B* 46:24907–18
Spiel DE. 1995. On the births of jet drops from bubbles bursting on water surfaces. *J. Geophys. Res.* 100:4995–5006
Spiel DE. 1997. More on the births of jet drops from bubbles bursting on seawater surfaces. *J. Geophys. Res.* 102:5815–21
Spiel DE. 1998. On the births of film drops from bubbles bursting on seawater surfaces. *J. Geophys. Res.* 103:24907–18

Stokes MD, Deane GB, Prather K, Bertram TH, Ruppel MJ, et al. 2013. A marine aerosol reference tank system as a breaking wave analogue for the production of foam and sea-spray aerosols. *Atmos. Meas. Tech.* 6:1085–94

Sullivan PP, McWilliams JC. 2010. Dynamics of winds and currents coupled to surface waves. *Annu. Rev. Fluid Mech.* 42:19–42

Tang IN, Tridico AC, Fung KH. 1997. Thermodynamic and optical properties of sea salt aerosols. *J. Geophys. Res. Atmos.* 102:23269–75

Textor C, Schulz M, Guibert S, Kinne S, Balkanski Y, et al. 2006. Analysis and quantification of the diversities of aerosol life cycles within AeroCom. *Atmos. Chem. Phys.* 6:1777–813

Thorpe SA. 1992. Bubble clouds and the dynamics of the upper ocean. *Q. J. R. Meteorol. Soc.* 118:1–22

Vaishya A, Jennings SG, O'Dowd C. 2012. Wind-driven influences on aerosol light scattering in north-east Atlantic air. *Geophys. Res. Lett.* 39:L05805

Veron F, Hopkins C, Harrison E, Mueller JA. 2012. Sea spray spume droplet production in high wind speeds. *Geophys. Res. Lett.* 39:L16602

Vignati E, Facchini MC, Rinaldi M, Scannell C, Ceburnis D, et al. 2010. Global scale emission and distribution of sea-spray aerosol: sea-salt and organic enrichment. *Atmos. Environ.* 44:670–77

Villermaux E. 2007. Fragmentation. *Annu. Rev. Fluid Mech.* 39:419–46

Villermaux E, Bossa B. 2009. Single-drop fragmentation distribution of raindrops. *Nat. Phys.* 5:697–702

Wang LP, Maxey MR. 1993. Settling velocity and concentration distribution of heavy particles in homogeneous isotropic turbulence. *J. Fluid Mech.* 256:27–68

Wu J. 1973. Spray in the atmospheric surface layer: laboratory study. *J. Geophys. Res.* 78:511–19

Wu J. 1992. Bubble flux and marine aerosol spectra under various wind velocities. *J. Geophys. Res.* 97:2327–33

Wu J. 1993. Production of spume drops by the wind tearing of wave crests: the search for quantification. *J. Geophys. Res.* 98:18221–27

Wu J. 1994. Film drops produced by air bubbles bursting at the surface of sea water. *J. Geophys. Res.* 99:16403–7

Wu J. 2001. Production functions of film drops by bursting bubbles. *J. Phys. Oceanogr.* 31:3249–57

Wu J. 2002. Jet drops produced by bubbles bursting at the surface of seawater. *J. Phys. Oceanogr.* 32:3286–90

Wu J, Murray JJ, Lai RJ. 1984. Production and distributions of sea spray. *J. Geophys. Res.* 89:8163–69

Zhao D, Toba Y, Sugioka K, Komon S. 2006. New sea spray generation function for spume droplets. *J. Geophys. Res.* 111:C02007

Annual Review of
Fluid Mechanics

Volume 47, 2015

# Contents

**Indexes**



**Errata**

An online log of corrections to *Annual Review of Fluid Mechanics* articles may be found at http://www.annualreviews.org/errata/fluid